The Geological Society of America
Special Paper 426
2007

Postglacial coastal evolution: Ice–ocean–solid Earth interactions in a period of rapid climate change

W.R. Peltier*
Department of Physics, University of Toronto, Toronto, Ontario M5S-1A7, Canada

ABSTRACT

The most recent glacial-interglacial transition of the late Pleistocene ice age was accompanied by an increase in globally averaged ice-equivalent eustatic sea level of ~120 m. This increase in sea level occurred over a period of ~10,000 yr and was accompanied by highly significant regional inundations of the land by the sea as well as by significant regional emergence of the land from the sea in the initially ice-covered regions. These migrations of the coastline can be accurately predicted given only an assumed known history of the deglaciation of the continents. An especially interesting aspect of the suite of physical interactions involved in the global process of glacial isostatic adjustment concerns the influence of variations in the Earth's rotation on the local histories of relative sea level, which may be inferred on the basis of radiocarbon dating of suitable sea-level index points. The observed variability in sea level may be interpreted in terms of fundamentally important climatological and solid Earth geophysical properties of Earth System processes that govern system evolution.

Keywords: glacial isostasy, relative sea level, Earth rotation.

INTRODUCTION

Understanding postglacial sea-level history has come to occupy a central position in modern research on Earth System evolution. The reasons for this are manifold but derive essentially from the fact that understanding of the processes that determine the evolving level of the sea as a function of space and time requires input not only from the "fluid earth sciences" of meteorology and oceanography but also from the "solid earth sciences" of geophysics and geology. It is therefore an area of research in which the concept of an "Earth System" of strongly interacting subcomponents is not only attractive intellectually but also mandatory to implement practically if significant understanding is to be achieved. My purpose in this paper is to illustrate and expand upon a number of the most recent advances that have been achieved in this area of research and to highlight some of the more important issues that remain.

The focus herein is centered upon the mathematical theory of Earth-ice-ocean interactions that has been developed and subjected to continuous refinement over the past three decades (see Peltier, 1998a for a recent detailed review). Of particular interest is the way in which, through the process of continuous refinement of this theory by the application of appropriate observational constraints, it has proven possible to achieve significant progress. From the point of view of solid Earth geodynamics, one of the most important contributions of this work has been the delivery of well-constrained models of the spherically averaged depth variation of the effective viscosity of the Earth's mantle. This Earth parameter is a required input to theories of the mantle convection process, which is responsible for driving the drift of the continents and the spreading of the seafloor away from the mid-ocean ridges. One of the few methods that may be employed to

*peltier@atmosp.physics.utoronto.ca

Peltier, W.R., 2007, Postglacial coastal evolution: Ice-ocean–solid Earth interactions in a period of rapid climate change, *in* Harff, J., Hay, W.W., and Tetzlaff, D.M., eds., Coastline Changes: Interrelation of Climate and Geological Processes: Geological Society of America Special Paper 426, p. 5–28, doi: 10.1130/2007.2426(02).

infer the magnitude and depth variation of this crucial parameter is through the formal inversion of observables related to the glacial isostatic adjustment process (Peltier 1998c).

From the point of view of climate dynamics in general and paleoclimatology in particular, an important contribution in this area has been in the delivery of well-constrained models of the space-time variations in continental ice cover and related paleotopography over the period since the Last Glacial Maximum (LGM), ~21.000 yr ago. The series of increasingly accurate models includes the ICE-1 model of Peltier and Andrews (1976), the ICE-2 model of Wu and Peltier (1982), the ICE-3G model of Tushingham and Peltier (1991), the ICE-4G model of Peltier (1994), and most recently the ICE-5G model of Peltier (2004). These models, beginning with the "4G" and "5G" global versions, have come to be heavily employed in the definition of the surface boundary conditions that are required in the application of modern coupled atmosphere-ocean general circulation models to the reconstruction of past states of the climate system (e.g., see Pinot et al., 1999 for a discussion of the use of the ICE-4G model in the context of the Paleoclimate Modeling Inter-comparison Project [PMIP]. This project is currently continuing as PMIP II, in which the group is employing the newest ICE-5G version of the reconstruction).

Given a well-constrained model of the internal visco-elastic structure of the planetary interior and an equally well-constrained model of the space-time history of the variation of surface ice cover, the mathematical theory of postglacial sea-level history may be employed to make predictions concerning the present-day rate of relative sea-level rise that would be expected to be measured as a secular drift of sea level on a tide gauge installed in any coastline region if the only process acting in the system were the process associated with the gravitational re-equilibration of the system following the elimination of ice from the continents that occurred during the most recent deglaciation event of the current ice age. As it happens, the contribution of this memory of surface deglaciation to modern tide gauge records is highly significant, as first noted in Peltier (1986). In Peltier and Tushingham (1989), an analysis was presented of a global data set of annually averaged tide gauge recordings from which the contamination associated with the influence of glacial isostatic adjustment was removed using the predictions of the theoretical model so as to more accurately infer the contribution to global sea-level rise due to the action of modern greenhouse gas–induced global warming. This analysis was further refined in Peltier (2001), who first produced the now widely accepted value for the rate of climate change–induced average rate of global sea-level rise of ~1.8 mm/yr that has been acting over the last half century of Earth history.

In the very recent past, two especially interesting issues have arisen in this area of research that will serve as primary focus in what is to follow. These are: (1) the net amount of ice that was melted from the continents during the most recent glacial-interglacial transition, and (2) the extent to which the process of rotational feedback influences relative sea-level histories through the Holocene interval of time, which extends from ~10,000 yr ago until the present. These issues have each somewhat polarized the community in recent years, and it will be my purpose here to address them both from the perspective of what can be said by combining the best possible observational constraints with the most recently refined theory. To this end, the next section of the paper will discuss the question of the latest observations concerning the volume of ice that must have been lost from the continents following the LGM. These data consist of an extended record from the island of Barbados in the Caribbean Sea derived from U/Th dated samples of various species of coral. The original record from this site, arguably the most important in the global archive, is that published by Fairbanks (1989). An extended version of this record has recently been published in Peltier and Fairbanks (2006), and this has proven crucial to more tightly constraining LGM global ice volume. As will be shown in the subsequent section of this paper, this extended Barbados record has allowed us (Peltier and Fairbanks, 2006) to fix the ice-equivalent eustatic rise of sea level across the transition from the glacial to the interglacial state to ~120 m, the number that has been traditionally inferred on the basis of deep-sea oxygen isotope data (e.g., Shackleton, 2000).

The second issue concerns the question of the impact of rotational feedback upon predicted Holocene histories of postglacial sea-level change. In recent years, several high-quality data sets have been collected that show Holocene relative sea-level history from coastlines located in what I have come to refer to as the "far field" of the main accumulations of LGM continental ice cover, and these may be employed to fully resolve the issue concerning the relative importance of this influence. The required analyses are also discussed, and a definitive test is described that has made it possible to isolate the precise nature of the sea-level signal associated with the Earth's rotational response to deglaciation. A summary of the results is offered in the last section, together with remarks concerning several of the remaining issues in this general area of research.

EXTENDED BARBADOS RECORD OF POSTGLACIAL SEA-LEVEL HISTORY

The island of Barbados, located in the eastern Caribbean Sea, ~150 km east of the Lesser Antilles, at 13°5′N latitude and 59°32′W longitude (Fig. 1), is a site from which an especially accurate U/Th record of the postglacial relative sea-level (RSL) history, from dated coral, has been available for some time (Fairbanks, 1989; Bard et al., 1990). Also shown on Figure 1 are the locations of the main concentrations of land ice that existed at the LGM according to the recently constructed ICE-5G(VM2) model (Peltier 2004), and the locations of several sites from which accurate records of Holocene sea-level history are available (which will be discussed in what follows). The original data set from Barbados has been significantly augmented (Fairbanks et al., 2005) since publication of these seminal accounts, and the newly available complete data set has been listed in Peltier and Fairbanks (2006). This data set is plotted on both Figure 2B and

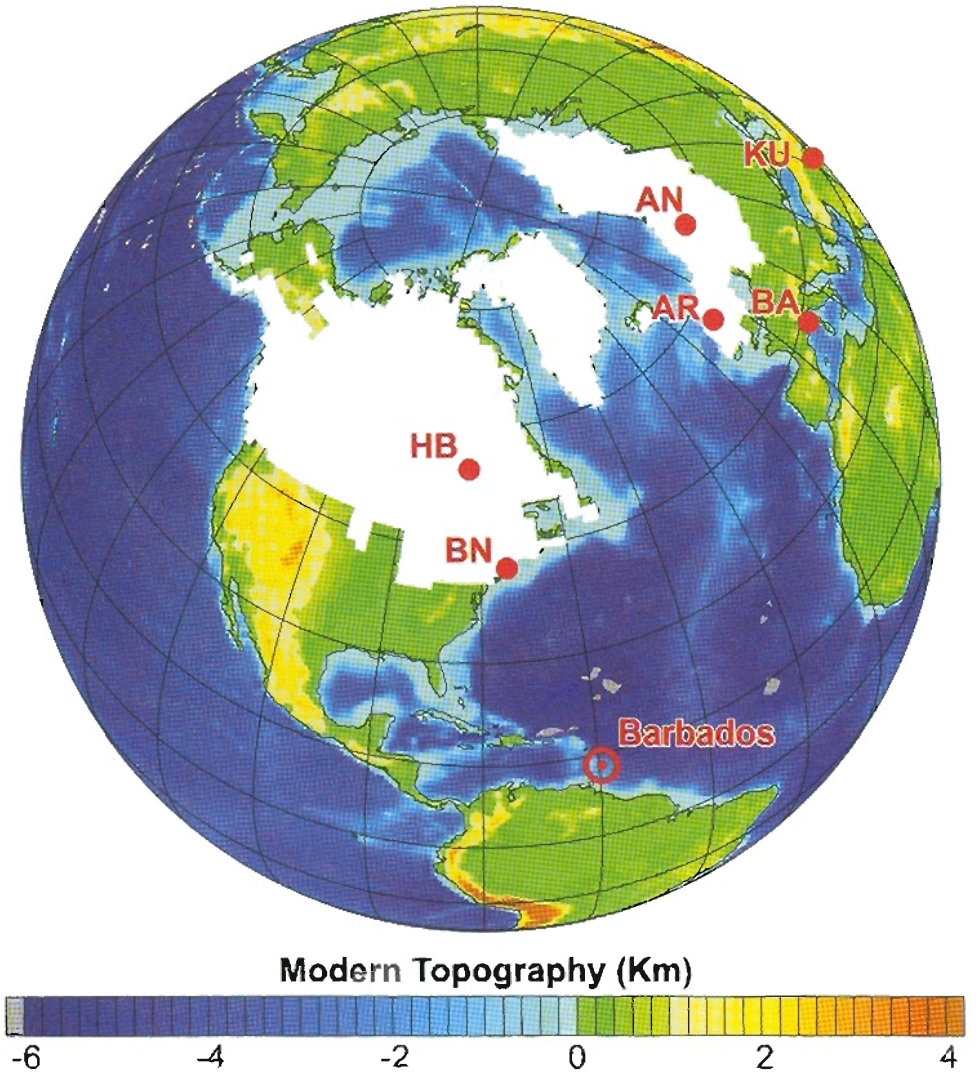

Figure 1. Location of the island of Barbados and several other sites from which relative sea-level records are available together with the location of the Northern Hemisphere continental ice sheets that existed at the Last Glacial Maximum. HB—SE Hudson Bay, BN—Boston, Massachusetts, Ar—Arisaig, AN—Angermanalven, BA—Baie des Anges, KU—Kuwait Bay.

Figure 3B as blue symbols consisting of a horizontal bar denoting the depth below sea level from which each coral sample was collected (corrected for an assumed rate of tectonic uplift of 0.34 mm/yr as discussed in Fairbanks, 1989), together with a vertical line extending upward from the horizontal bar, the length of which denotes the range of depths below sea level within which the specific species of coral could live. The coral-derived sea-level index points in this data set are provided by four different species of coral, respectively, *Acropora palmata* (Ap), *Montastrea annularis* (Ma), *P. asteroides* (Pa), and *Diploria* (Di). As recently discussed in Peltier and Fairbanks (2006, p. 3325), "the most important index points are provided by the Ap measurements since the Ap facies, i.e., the reef zone numerically dominated by the reef crest species Ap, is restricted to a water depth within 5 m of sea-level in the modern ecology (Fairbanks, 1989, as shown by the short error bars attached to them in Fig. 2). Observations of isolated Ap colonies or storm-displaced specimens deeper than 5 m have been reported, but to our knowledge, Ap specimens collected from the Ap facies can be reliably assigned to 5 m or shallower water depths. However, the data derived from *M. annularis*, indicated by error bars of an intermediate length of 20 m, are actually of considerable value as well." Since the living depths of the other species are not adequately restricted (long error bars), they provide only a lower limit upon relative sea-level history at this location.

Also shown on Figures 2B and 3B is the eustatic sea-level curve for the ICE-5G(VM2) model of the global process of glacial isostatic adjustment of Peltier (2004). This curve is shown

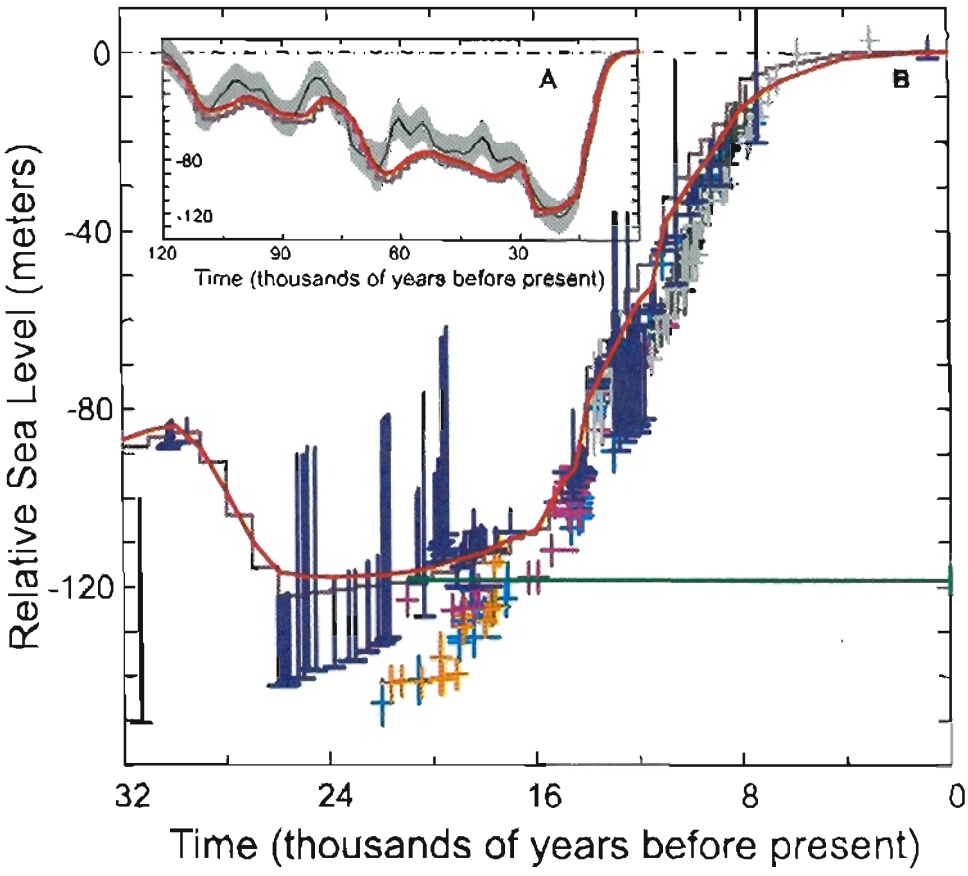

Figure 2. (A) The deep-sea oxygen isotope–derived global eustatic sea-level curve of Waelbroeck et al. (2002) shown as the thin black line with error bars represented by the surrounding shaded region. Also shown is the predicted relative sea-level history at the island of Barbados using the ICE-5G(VM2) model of the last glacial-interglacial cycle (red curve) and the "ice equivalent" eustatic sea-level history of the ICE-5G model of global deglaciation (purple "step-discontinuous" curve). (B) The extended Barbados record of late glacial and deglacial relative sea-level history shown by the blue symbols for which the horizontal bars denote the depths from which the samples were actually recovered, corrected for an assumed rate of tectonic uplift of 0.34 mm/yr. The vertical line attached to the horizontal bars denotes the range of depths below sea level within which the individual species of coral may live. The samples with the shortest attached error bars (of length 5 m) are those of the species *Acropora palmata*; those with the attached error bars of the intermediate length (20 m) are those of the species *Montastrea annularis*, whereas those with the longest attached error bars are those of species that provide only lower bounds upon sea level by virtue of the very great depth below the level of the sea at which they may live. The red curve shows the predicted relative sea-level history at Barbados according to the ICE-5G(VM2) model of the global process of glacial isostatic adjustment, and the purple "step-discontinuous" curve shows the "ice-equivalent" eustatic sea-level history of the ICE-5G model of the glaciation-deglaciation process. The colored crosses are the data points selected to define the ice-equivalent eustatic sea-level history according to Lambeck and Chappell (2001). The color code employed for these data is as follows: cyan (Barbados), gray (Tahiti), black (Huon), orange (Bonaparte Gulf), purple (Sunda Shelf).

as the purple step-discontinuous line on each of these figures. In Figure 2B, this line has been computed by first calculating the volume of ice V_I that is assumed to have melted at a given instant of time in the model and converting this to the volume V_w of water thereby produced based upon the assumption of mass conservation, which gives $V_w = V_I(\rho_I/\rho_w)$, where ρ_I and ρ_w are the densities of ice and water, respectively. The "ice-equivalent" eustatic sea-level increment at this instant of time is then computed as $\Delta S_{eustatic} = V_w / A_O$, where A_O is the assumed constant surface area of the oceans, which is taken to be equal to the present-day area. The purple eustatic curve shown on Figure 2B is termed "ice equivalent" because it is not influenced at all by the time dependence of the actual surface area of the oceans caused by coastline migration. In contrast, the purple step-discontinuous curve

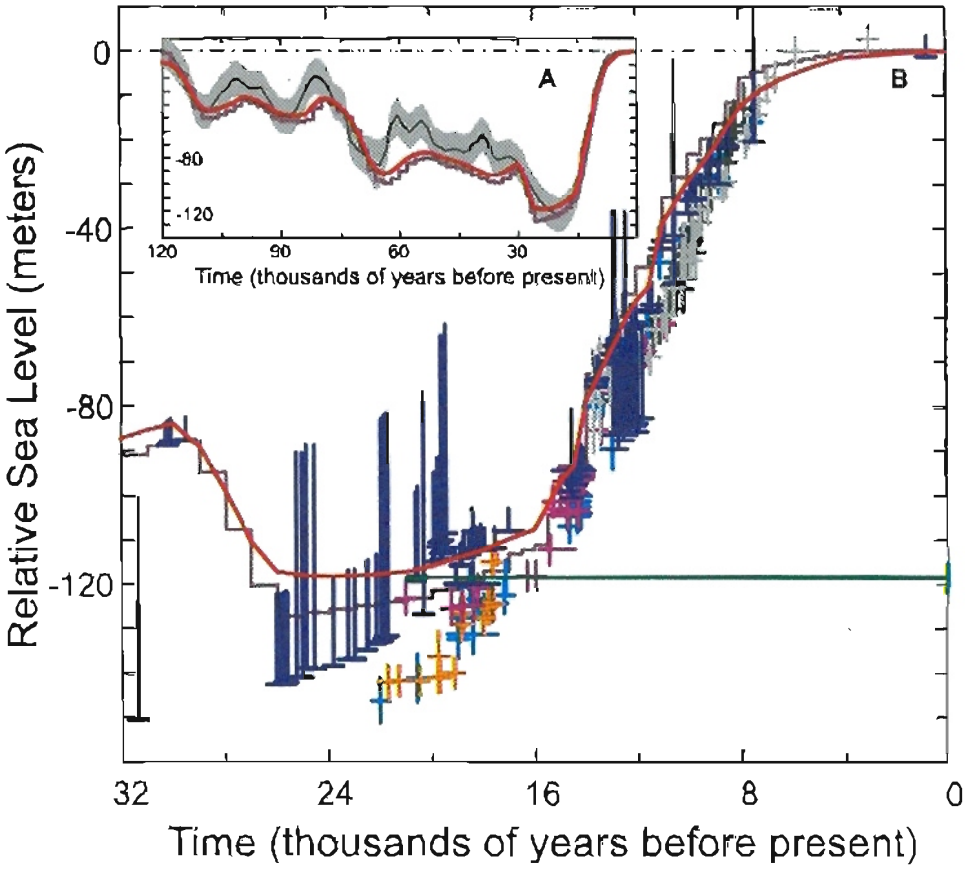

Figure 3. Same as Figure 2 except the eustatic curve shown in both A and B includes the influence of the time dependence of the surface area of the oceans so that this eustatic sea-level history is not "ice equivalent."

shown on Figure 3B cannot be termed "ice equivalent" because it does include the contribution to the change of sea level due to the changing surface area of the oceans that occurs due to coastline migration. Since the amount by which the surface area of the oceans changes in a given time step depends upon the visco-elastic model of the Earth used to model the glacial isostatic adjustment process, the incorporation of this influence upon the eustatic curve means that the curve so produced is not solely dependent upon the loss or gain of grounded continental ice. This influence causes the LGM "eustatic" depression of the sea to be greater than the "ice-equivalent eustatic" depression because the LGM surface area of the oceans was smaller at this time than it is at present. Intercomparison of the two "eustatic" curves for the ICE-5G model of the global deglaciation process with the actual Barbados observations demonstrates that both fit the actual sea-level observations rather well, although the "eustatic" curve that includes the influence of time dependence of the surface area of the oceans lies somewhat below the data in the LGM interval of time.

The red curves shown on both Figures 2B and 3B are the predictions of the theoretical model of the global process of glacial isostatic adjustment of the relative sea-level history that should be observed at the Barbados location based upon the ICE-5G(VM2) model of Peltier (2004). These curves are of course identical because the theoretical model fully accounts for the process of coastline migration, as will be discussed explicitly in the following section of this paper. It is important to note that the red curve on Figure 2B quite accurately overlaps the purple discontinuous "ice-equivalent" eustatic curve of the ICE-5G model of the deglaciation of the continents. By comparing the red-predicted and purple-eustatic curves on Figure 3B, however, it is evident that there is some misfit during the LGM: the relative sea-level prediction lies somewhat above the eustatic curve that includes the influence of the changing surface area of the oceans. The main point shown on Figures 2B and 3B is that the observed relative sea-level history at the island of Barbados itself provides an accurate measurement of the "ice-equivalent" eustatic variation of sea level that has occurred since the LGM. This fact was first pointed out in Peltier (2002a) in connection with analyses performed on the basis of the previous ICE-4G model of the deglaciation process. The ice-equivalent eustatic depression of global sea level during the LGM, accord-

ing to this analysis, was therefore very close to the 120 m estimate conventionally derived on the basis of deep-sea oxygen isotopic records, as recently discussed in Shackleton (2000). This level is marked on both Figures 2B and 3B by the horizontal green line.

Also shown on both Figures 2B and 3B are the data points, shown as colored symbols, that were taken to define the "ice-equivalent" eustatic sea-level curve of Lambeck and Chappell (2001). The data employed to define their curve included a number of additional coral-based records, including those from the Huon Peninsula of Papua New Guinea of Chappell et al. (1996), as well as those from Tahiti of Bard et al. (1996). Since neither of these records extends to the LGM, they are of no help in defining the depth of the LGM sea-level lowstand. They are furthermore compromised, especially the Huon record, by the poorly constrained nature of the rate of tectonic uplift or subsidence that must be employed to decontaminate the raw measurements in order to infer past sea levels (see Peltier, 1998a, for detailed discussion). The observations employed by Lambeck and Chappell (2001) to define the LGM sea-level lowstand included data from the J. Bonaparte Gulf of northern Australia described in Yokoyama et al. (2000) as well as data from Barbados and from the Sunda Shelf of Indonesia from Hanebuth et al. (2000). Figure 4 shows the predictions of relative sea-level history for both the Sunda Shelf and J. Bonaparte Gulf locations using the same ICE-5G(VM2) model that so well fits the Barbados observations. This figure shows predictions that both include and exclude the influence of rotational feedback (Figs. 4B and 4C) and the locations of the sites from which the sedimentary cores were raised that contained the sea-level index points employed. The predictions that exclude this rotational influence are shown in black, whereas those that include the influence are shown in red. (The red curves shown on Figures 2B and 3B also included the influence of rotational feedback.) As seen in Figure 4, the model fits the record from the Sunda Shelf very well, but there is a substantial misfit to the data from J. Bonaparte Gulf, if the data points shown as colored symbols are accepted as accurate measurements of relative sea level. These samples may have been significantly reworked, as suggested by Shennan and Milne (2003). By comparing the supposed ice-equivalent sea-level index points of Lambeck and Chappell (2001) with the results shown on Figure 4 for the J. Bonaparte Gulf, it can be established that their conversion of the observed depths of the sea-level index points from the J. Bonaparte Gulf to obtain an LGM "ice-equivalent eustatic" sea-level lowstand involved a 20 m shift of the data to increased depth. This shift appears to be connected to the assumption of the existence of a 19 ka meltwater pulse by Yokoyama et al. (2000), the existence of which was questioned in Peltier (2002b). In that paper attention was also drawn to a flaw in the methodology employed by this group which led to the retraction published in Yokoyama et al. (2001).

Most important from the present perspective is the fact that the extended set of Barbados data discussed in Peltier and Fairbanks (2006) can rule out the occurrence of the strong meltwater pulse at 19 ka hypothesized by Yokoyama et al. (2000) on the basis of the data from J. Bonaparte Gulf. Prior to the availability of this extended record, the occurrence of such an event could not be excluded on the basis of the Barbados record because all of the samples in the data set older than 19,000 yr were of the coral species *Montastrea annularis*, and these were recovered from a depth that allowed the possibility of such an event, as discussed in Peltier (2002b). The extended data set, however, includes samples that extend to the conventional LGM age of 21 ka, and the depths from which these samples were raised are such as to firmly reject the 19 ka meltwater pulse hypothesis. In plotting the Barbados samples shown as the colored symbols on Figures 2B and 3B, Lambeck and Chappell (2001) elected to plot them without the properly attached error bar of 20 m length that actually represents the range of depths over which these corals may exist (see Peltier and Fairbanks, 2006, for further discussion). Instead, they plotted these samples as though they provided, based upon the depth below sea level from which they were actually extracted, firm constraints upon the relative level of the sea. However, as is clear on the basis of either Figure 2B or 3B, this species of coral is often found at the shallowest portion of its depth range rather than the deepest portion. This is clear on the basis of the numerous samples of this species of Younger Dryas age that all lie ~20 m below the depth of *Acropora palmata* samples of the same age. The deep LGM lowstand characteristic of the Lambeck and Chappell (2001) reconstruction of "ice-equivalent" eustatic sea level is therefore constrained only by the improperly adjusted depth data from J. Bonaparte Gulf and, in particular, by the hypothesized 19 ka meltwater pulse, which has been firmly rejected by the extended Barbados data set. This data set fixes this measure of LGM continental ice volume near the vicinity of the conventional value of 120 m.

Also shown in part A of Figures 2 and 3 is the ice-equivalent eustatic sea-level reconstruction of Waelbroeck et al. (2002), which is shown as the thin black line with the error in the reconstruction indicated by the shaded region surrounding this best estimate. This reconstruction was based primarily upon oxygen isotopic measurements from deep-sea sedimentary cores corrected for the influence of variations in abyssal ocean temperature. Data based upon the coral records were also assimilated into this interpretation. Inspection of this record also shows it to be characterized by an LGM sea-level lowstand very near to 120 m. Also included in this figure are the predicted history of relative sea-level change at Barbados and the ice-equivalent eustatic curve for the ICE-5G model for the entire last glacial-interglacial cycle. It can be observed that even on the time scale of the entire 100,000 yr period, the records are in very close accord. There is some systematic misfit between the Waelbroeck et al. eustatic curve and that of the ICE-5G model during the glaciation phase of the cycle. This misfit is due to the fact that the SPECMAP record of Imbrie et al. (1984) was employed to constrain this portion of the ICE-5G reconstruction. In the future, this early portion of the integrated ice-volume history will be adjusted to better conform to that delivered by the Waelbroeck et al. (2002) analysis.

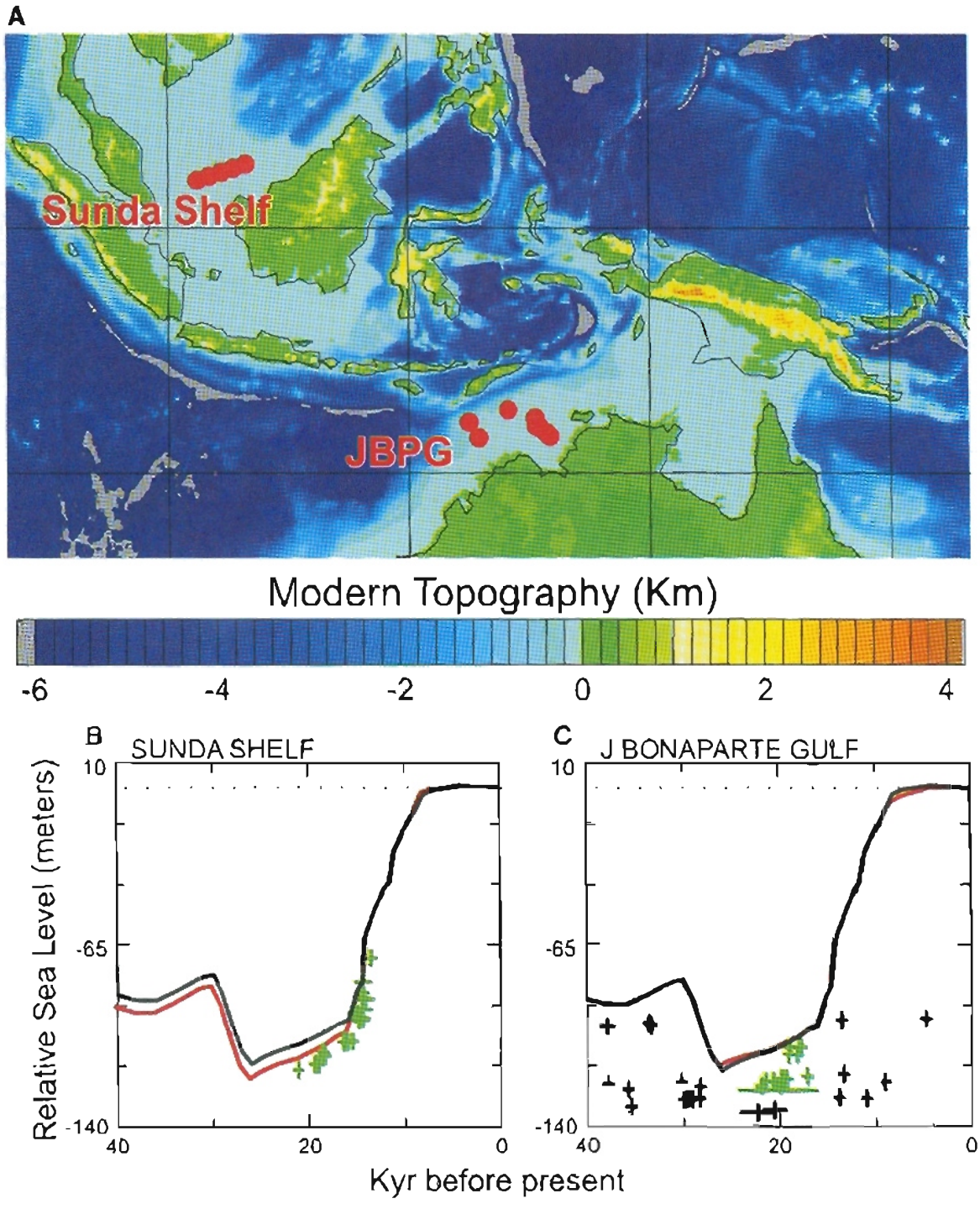

Figure 4. (A) The geographical locations of the sedimentary cores from which the sea-level index points were extracted to define the history of sea-level variations at both the Sunda Shelf and J. Bonaparte Gulf (JBPG). The positions of these cores are shown superimposed upon the modern bathymetry. (B and C) Comparisons of the inferred and predicted relative sea-level histories at the J. Bonaparte Gulf and Sunda Shelf locations based upon use of the ICE-5G(VM2) model. Two predictions for each site are shown using this model: one that includes the influence of rotational feedback (red curve) and another that omits this influence (black curve).

There is one further piece of information to note concerning the ice-equivalent eustatic lowstand of the sea. This is the contribution of Siddall et al. (2003) based upon the analysis of oxygen isotopic data derived from Red Sea sedimentary cores. These authors analyzed the impact on the "exchange flow" of water across the sill at the entrance to the Red Sea as a function of the changing depth of the water above the sill that occurred during the sea-level variations associated with the most recent glaciation cycle. The strength of this exchange flow significantly modulates the impact that evaporation has upon the salinity of the water in this inland sea, and the analysis has enabled inferences to be made about the magnitude of sea-level changes that have occurred during the glaciation-deglaciation process. Although their reconstructions also show that local sea level was depressed by a maximum of 120 m at the LGM, it is not clear that this has allowed any independent measure of the "ice-equivalent" eustatic depression at LGM because a full account has not been taken of the local impact of the isostatic adjustment process (some discussion of this impact has, however, appeared in Siddall et al., 2004). Further analysis of this interesting data set using more complete models of the fluid mechanics of the exchange flow over the sill would be extremely useful.

THEORY OF POSTGLACIAL RELATIVE SEA-LEVEL HISTORY AND THE IMPACTS OF EARTH ROTATION AND COASTLINE MIGRATION

The origins of the modern theory of postglacial sea-level change employed for the predictions of postglacial relative sea-level history described in the last section are to be found in a series of papers that appeared almost 30 yr ago (Peltier, 1974, 1976; Peltier and Andrews, 1976; Farrell and Clark, 1976; Clark et al., 1978; Peltier et al., 1978). This theory has been significantly further enhanced, and some of the enhancements were reviewed in Peltier (1998). The theoretical prediction of relative sea-level history, $S(\theta, \lambda, t)$, in which θ is latitude, λ is longitude, and t is time, is obtained as a solution to the following integral equation:

$$S(\theta,\lambda,t) = C(\theta,\lambda,t)\left[\int_0^t dt' \iint_\Omega d\Omega' \left\{ L(\theta',\lambda',t') G^L(\gamma, t-t') + T(\theta',\phi',t) G^T(\gamma, t-t') \right\} + \frac{\Delta\Phi(t)}{g}\right]. \quad (1)$$

In this equation $C(\theta, \lambda, t)$ is the ocean function, which is by definition unity over the oceans and zero over the continents. This is an integral equation because the surface mass load per unit area, L, has the following composite form:

$$L(\theta,\lambda,t) = \rho_i I(\theta,\lambda,t) + \rho_w S(\theta,\lambda,t), \quad (2)$$

in which ρ_i and ρ_w are the densities of continental ice and ocean water, respectively, and $I(\theta, \lambda, t)$ is the time- and space-dependent thickness of ice on the continents. It is because S appears both on the left-hand side of Equation 1, and also as a component of the integrand of the triple convolution integral on the right-hand side, that the equation is an integral equation. The remaining terms in Equation 1 include $G^L(\gamma, t)$, which is the Green function for separation between the surface of the assumed spherically symmetric Maxwell visco-elastic model of the solid Earth (e.g., see Peltier, 1974) and the equipotential surface of the sea (γ is the angular separation between source point and field point), which has the form:

$$G^L(\gamma,t) = \frac{\varphi(\gamma,t)}{g} - \Gamma(\gamma,t), \quad (3)$$

in which $\varphi(\gamma, t)$ is the perturbation of the gravitational potential and $\Gamma(\gamma, t)$ is the perturbation of the local radius of the solid Earth induced by a point mass load that is applied to the surface at $t = 0$ and is instantaneously removed. The mathematical methods required to compute the elements of the composite Green function $G^L(\gamma, t)$, namely Γ and ϕ, were first presented in Peltier (1974) and Peltier and Andrews (1976), respectively. The further terms in Equation 1, T and G^T, denote the perturbation to the centrifugal potential due to the alteration of the rotational state of the planet caused by the isostatic adjustment of its shape and internal mass distribution, and the Green function for the separation between the surface of the solid Earth and the equipotential surface of the sea that is induced by this applied variation of potential, respectively. The required theory for the change in rotation due to the glacial isostatic adjustment (GIA) process was first presented in Peltier (1982) and Wu and Peltier (1984), while the theory for the incorporation of the influence of rotational feedback onto sea level (at the level of first-order perturbation theory) was first described in Peltier (1998, 1999). The explicit form for the perturbation to the centrifugal potential required to compute the impact of rotational feedback onto sea level through the solution of Equation 1 may be derived following Dahlen (1976), whose analysis led to the following form for the function T:

$$T = T_{00} Y_{00} + \sum_{m=-1}^{+1} T_{2m} Y_{2m}(\theta,\lambda), \quad (4)$$

in which Y_{lm} are spherical harmonics of degree l and order m, and the required expansion coefficients T_{lm} are as follows:

$$T_{00} = \frac{2}{3}\omega_3(t)\Omega_0 a^2, \quad (5a)$$

$$T_{20} = -\frac{1}{3}\omega_3(t)\Omega_0 a^2 \sqrt{4/5}, \quad (5b)$$

$$T_{21} = \left[\omega_1(t) - i\omega_2(t)\right]\left(\Omega_0 a^2/2\right)\sqrt{2/15}, \quad (5c)$$

$$T_{2-1} = -\left[\omega_1(t) + \omega_2(t)\right](\Omega_0 a^2/2)\sqrt{2/15}. \quad (5d)$$

in which the variables $\omega_i(t)$ are the perturbations to the three Cartesian components of the angular velocity vector of the planet caused by the exchange of mass between the continents and the oceans associated with the glaciation-deglaciation process. In what follows, it will prove important to understand that the component $\omega_3(t)$ is the increment (when positive) to the angular velocity of rotation about the axis of greatest inertia, and therefore this variable controls the variation in the length of day associated with the glacial isostatic adjustment process. On the other hand the components $\omega_1(t)$and $\omega_2(t)$ control the "wander" of the pole of rotation relative to the surface geography. It is this polar wander effect that has the greatest influence upon sea-level history. The remaining variables in Equations 5a–5d consist of the rate of axial rotation of the planet in its unperturbed state, Ω_0, and Earth's radius, a. Computation of the time series for the $\omega_i(t)$ employs the theory described in Peltier (1982) and Wu and Peltier (1984), which requires the construction of a detailed model of the temporal variations in each of the elements of the moment of inertia tensor caused by the glaciation-deglaciation process.

Attention has recently been drawn to the importance of the influence of rotational feedback upon observed Holocene relative sea-level histories in Peltier (2002c) and Peltier (2005). It has been shown that this feedback is required to understand the anomalous sea-level highstands observed along the south coast of Argentinian Patagonia, and the strength of the feedback embodied in the ICE-4G(VM2) and ICE-5G(VM2) models of the glacial isostatic adjustment process leads to a correct prediction of the highstands documented in Rostami et al. (2000). This idea will be further explored in the following section of this paper.

The final term in Equation 1, $\Delta\Phi(t)/g$, was first discussed in Farrell and Clark (1976) using the mathematical solution for $G^L(\gamma, t)$ appropriate for a particular linearly visco-elastic Maxwell model of Earth derived from the work presented in Peltier (1974) and Peltier and Andrews (1976). This term is determined based upon the requirement that the glacial isostatic adjustment process must conserve mass, i.e., that the mass of ice that is melted from the continents equals the mass of water that enters the ocean basins. The first solutions to Equation 1 were presented in Clark et al. (1978) and Peltier et al. (1978) together with comparisons of these theoretical predictions to observations of relative sea-level change through the Holocene epoch (most recent 10,000 yr) of Earth history, observations for which chronological control was provided by ^{14}C dating of the pertinent sea-level index points. Even these earliest intercomparisons of theory and observations demonstrated that the theory appeared to capture all of the most essential spatial variability contained in Holocene observations. Especially important was the fact that the gravitationally self-consistent nature of the theory led to a direct prediction of the occurrence of the mid-Holocene sea-level highstands that had been observed to be a characteristic of relative sea-level histories at all oceanic islands in the equatorial Pacific Ocean.

The methodology presented herein is a further refinement of that described recently in Peltier (2005), which includes a method for the solution of Equation 1 that is especially well suited for computation of sea-level histories when a complete cycle of glaciation and deglaciation is employed for continental ice-sheet history, even in circumstances in which the land-sea interaction is as complex as that described in Tarasov and Peltier (2004). This methodology begins by invoking the globally accurate algorithm for the computation of the time dependence of the ocean function $C(\theta, \lambda, t)$ that was first presented in Peltier (1994, 1996) and that remains central in order for the refined method for the solution of Equation 1 to be employed for present purposes. We begin by first rewriting Equation 1 in the schematic form, following the discussion in Peltier (2005), as:

$$S(\theta,\lambda,t) = V(\theta,\lambda,t) + D(t), \tag{6}$$

from which the explicit appearance of the multiplicative factor C has been eliminated because the field S is defined everywhere over the surface of the planet, even where there is no ocean. The function $S(\theta, \lambda, t)$ of latitude, longitude, and time is simply the perturbation of the height of the geoid (the surface of constant gravitational potential that is coincident with the surface of the sea where ocean exists) relative to the surface of the solid Earth. Now Equation 6 may be solved discretely in time using the iterative procedure described in detail in Peltier (1998a), in which the full influence of rotational feedback on sea-level history is incorporated. Suppose that we consider the change in sea level between the $n-1$ time step and the nth time step. If $C_n = C_{n-1}$, then the change in the thickness of the water load at a given point on the surface, and thus relative sea level, would simply be $(S_n - S_{n-1})C_n$. However, if $C_n \neq C_{n-1}$, then the change in water load will not be accurately estimated by this expression at those locations where C_n differs from C_{n-1} because of coastline migration.

In fact, there are several sources of error that arise due to the temporal evolution of C, sources that act within the interior of the zone where initially glaciated regions later become inundated by the sea (or vice versa), and a source in those locations outside the zones of glaciation in which, for example, initially exposed continental shelf is being inundated by the sea due to the melting of continental ice. Both of these sources of error were explicitly recognized in Peltier (1998a). In previous work on the influence of time-dependent ocean function, these two regions were treated separately. In particular, the interior region was addressed by accounting for the action of "implicit ice" in Peltier (1998b), and the exterior region has been dealt with by recognizing the influence of a "broad shelf effect" (Peltier and Drummond, 2002).

The form of this algorithm to be employed herein is a further enhancement of that reported in Peltier (2005) and first employed in Peltier and Fairbanks (2006). In this form of the algorithm the interior and exterior regions in which C varies are treated simply by storing the increment in sea-level S_{n-1} obtained in the previous time step in the iterative solution of Equation 1 as well as the form of the ocean function, C_{n-1}, and paleotopography T_{n-1} obtained at the same time. We then compute the actual sea-level change in the regions of changing C by using expressions that define the volume of the ocean lost or gained between the evolv-

ing paleotopography and the equipotential surface of the sea. As discussed in detail in Peltier and Fairbanks (2006), this leads to a prediction of the space-dependent increment in sea level between time-step $n-1$ and time step n that very accurately accounts for the mass conservation constraint. The results presented herein were obtained using this further refined form of the algorithm employed to solve Equation 1.

Figure 5 shows the fit of the predictions of the ICE-5G(VM2) model to observed Holocene records of postglacial relative sea-level history at eight different geographical locations, with the sites of the individual relative sea-level observations shown superimposed upon a global map of the model-predicted present-day rate of sea-level rise. The sources of the Holocene relative sea-level data plotted in each of the eight intercomparisons are provided in the list of references at the end of this paper. For each location, the results of two different versions of the ICE-5G(VM2) model are shown. One of these is the same version of the model that I refer to as version 1.2 which posits the occurrence of the Last Glacial Maximum at 26,000 yr ago rather than the conventionally assumed age of 21,000 yr. Peltier and Fairbanks (2006) presented a defense of this suggested revision to the time at which the greatest concentration of land ice existed. The second prediction shown for each site on Figure 5 is based upon the original ICE-5G model as published in Peltier (2004), in which the conventional LGM age of 21,000 yr was assumed.. Inspection of the comparisons between theoretically predicted and geologically inferred relative sea-level histories demonstrates that the model reasonably reconciles this set of observations at all locations over the Holocene period. It should be understood that the data at ice-sheet–centered sites, such as SE Hudson Bay in Canada and Angerman River in Sweden, have been employed to tune the model for both ice-sheet thickness and the radial profile of mantle viscosity (e.g., see Peltier, 1982, 1998a, for detailed discussion).

THE INFLUENCE OF ROTATIONAL FEEDBACK UPON POSTGLACIAL RELATIVE SEA-LEVEL HISTORY

Inspection of Figure 4, which shows comparisons between the predictions of postglacial sea-level history for the Sunda Shelf location with the observations of Hanebuth et al. (2000), has already established the importance of rotational feedback in verifying the validity of the ICE-5G(VM2) model of the global process of glacial isostatic adjustment. In the absence of the incorporation of this effect, it is clear that the model that so well fits the Barbados record does not fit the record at the Sunda Shelf. When this effect is included, however, the theoretical prediction fits the data from this location rather well, especially given the fact that the data that define the LGM lowstand at this site are expected to lie somewhat below the actual level of the sea in this interval of time. Given the importance of the influence of this feedback effect for the purpose of model validation, it is clearly important to further establish the accuracy of the theoretical methodology that has been employed to predict its magnitude. Here, I discuss a new series of analyses used to verify that the theory has the accuracy required by the quality of the observational constraints available.

In order to better understand the validation tests, Figure 6 provides an initial insight. This figure shows, in Mollwiede projection, predictions of the present-day rate of relative sea-level rise for four different versions of the theoretical model. Results are shown for both ICE-4G(VM2) and ICE-5G(VM2) models, both including and excluding the influence of rotational feedback. It is clear by inspections of these color maps that incorporation of the influence of rotational feedback superimposes a modification that has the form of a degree 2 and order 1 spherical harmonic upon the space-dependent predictions of this rate of change. In particular the predicted rates of change are made more negative in regions centered upon the southern tip of the South American continent and over the Japanese islands, and predicted rates of change are made more positive in regions centered over the Pacific Ocean south of the Australian continent and over but somewhat offshore of the northeast coast of the North American continent. Furthermore, it is clear by inspection of the figure that the degree 2 and order 1 component of the pattern is stronger in the prediction of the ICE-5G(VM2) model than it is in the ICE-4G(VM2) model. The dominance of the impact of rotational feedback by a pattern of degree 2 and order 1 form is clearly associated with the dominance of the influence of the polar wander effect, as is clear by inspection of Equations 5a–5d.

The spatial orientation of the degree 2 and order 1 pattern may be seen more clearly simply by subtracting the prediction that excludes this influence from the prediction of the present-day rate of sea-level rise that includes this influence. Figure 7 shows the results of such an analysis for the ICE-5G(VM2) model. Figure 7A shows the former and Figure 7B the latter prediction. The difference is shown in Figure 7C. Since the predicted influence of the polar wander effect reaches an extremum in four different regions, it would seem reasonable to seek verification of the accuracy of the theoretical prediction of this influence by analysis of relative sea-level data from within these regions. The database of relative sea-level histories that my students and I have compiled at the University of Toronto includes over 600 ^{14}C-dated relative sea-level histories, many of which are from sites within the four extrema of the spherical harmonic degree 2 and order 1 pattern associated with the influence of rotational feedback. Locations of the best available sites are superimposed upon each of the maps in Figure 7. All of these locations have been selected from within the four extrema, but, in the case of that over the northeast coast of the North American continent, only sites well removed from the region of heavy ice cover have been selected. The latter region turns out not to be as useful for our purposes as the other three, a consequence of the fact that it lies in the "near field" of the Laurentide ice sheet and is therefore most strongly influenced by the direct effect of postglacial rebound of the crust. Because the influence of rotational feedback is a subtle effect, it turns out to be most clearly visible at sites well removed from the main centers of deglaciation.

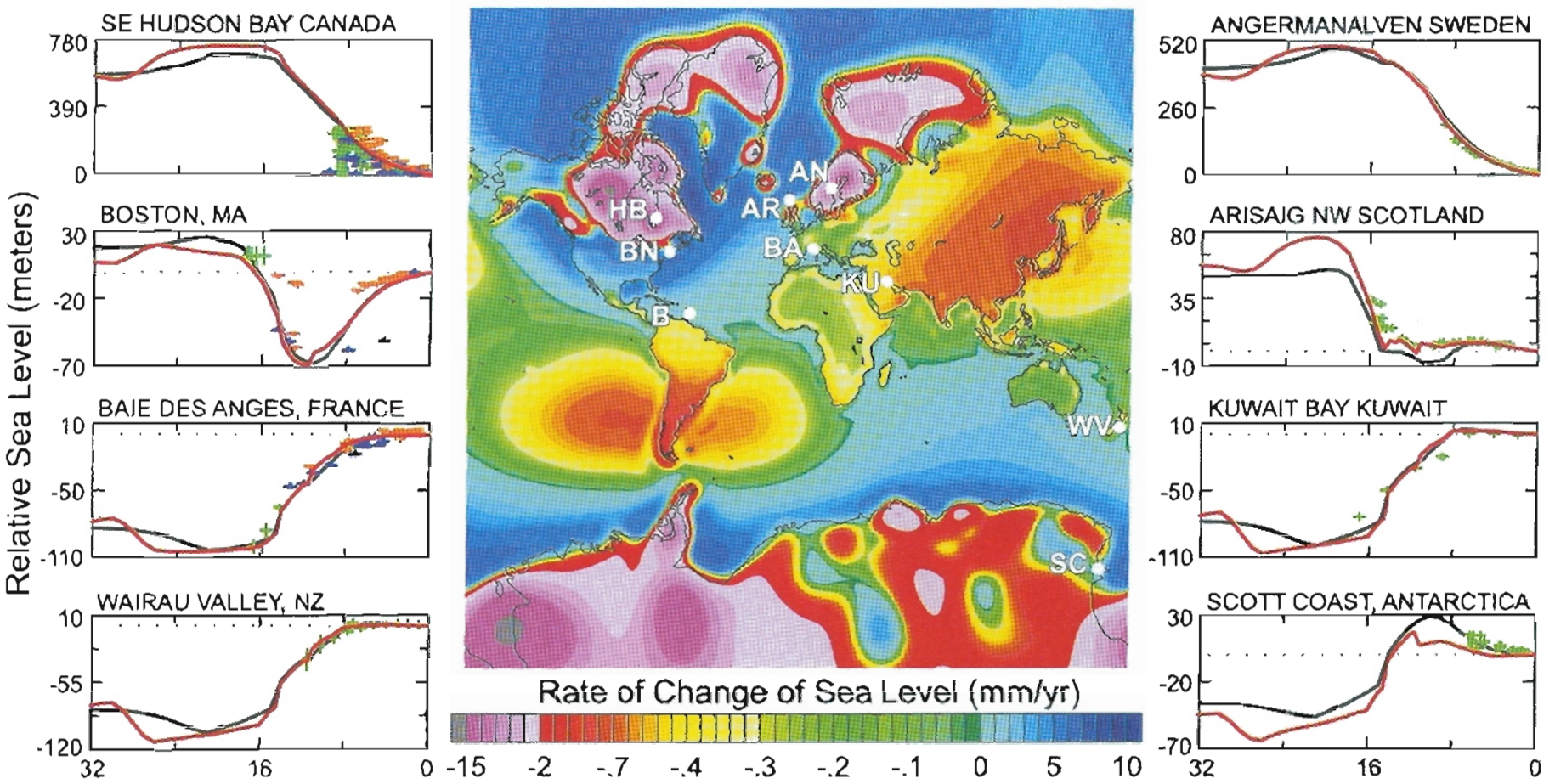

Figure 5. Intercomparisons between observed and predicted relative sea-level histories at eight different geographical locations using two different versions of the ICE-5G(VM2) model of the deglaciation process, versions 1.1 and 1.2, respectively. In version 1.1, the Last Glacial Maximum (LGM) was assumed to have occurred at the conventional age of 21 ka. In version 1.2, LGM is assumed to have occurred earlier, at 26 ka. The positions of the eight sites are shown in the central part of the figure superimposed upon a Mercator projection of the present-day predicted rate of relative sea-level rise that would be expected to be observed on a long-tide gauge recording if the only process acting in the system were that associated with the most recent glacial cycle of the late Pleistocene ice age. The references and abbreviations are as follows: SE Hudson Bay, Canada (HB; Peltier, 1998a); Boston, Massachusetts (BN; Kaye and Barghoorn, 1964); Baie des Anges, France (BA; Dubar and Anthony, 1995); Wairau Valley, New Zealand (WV; Pickrill, 1976); Angermanalven, Sweden (AN; Cato, 1992); Arisaig, Scotland (AR; Shennan et al., 1993); Kuwait Bay (KU; Al-Asfour, 1982); Scott Coast (SC; Hall and Denton, 1999).

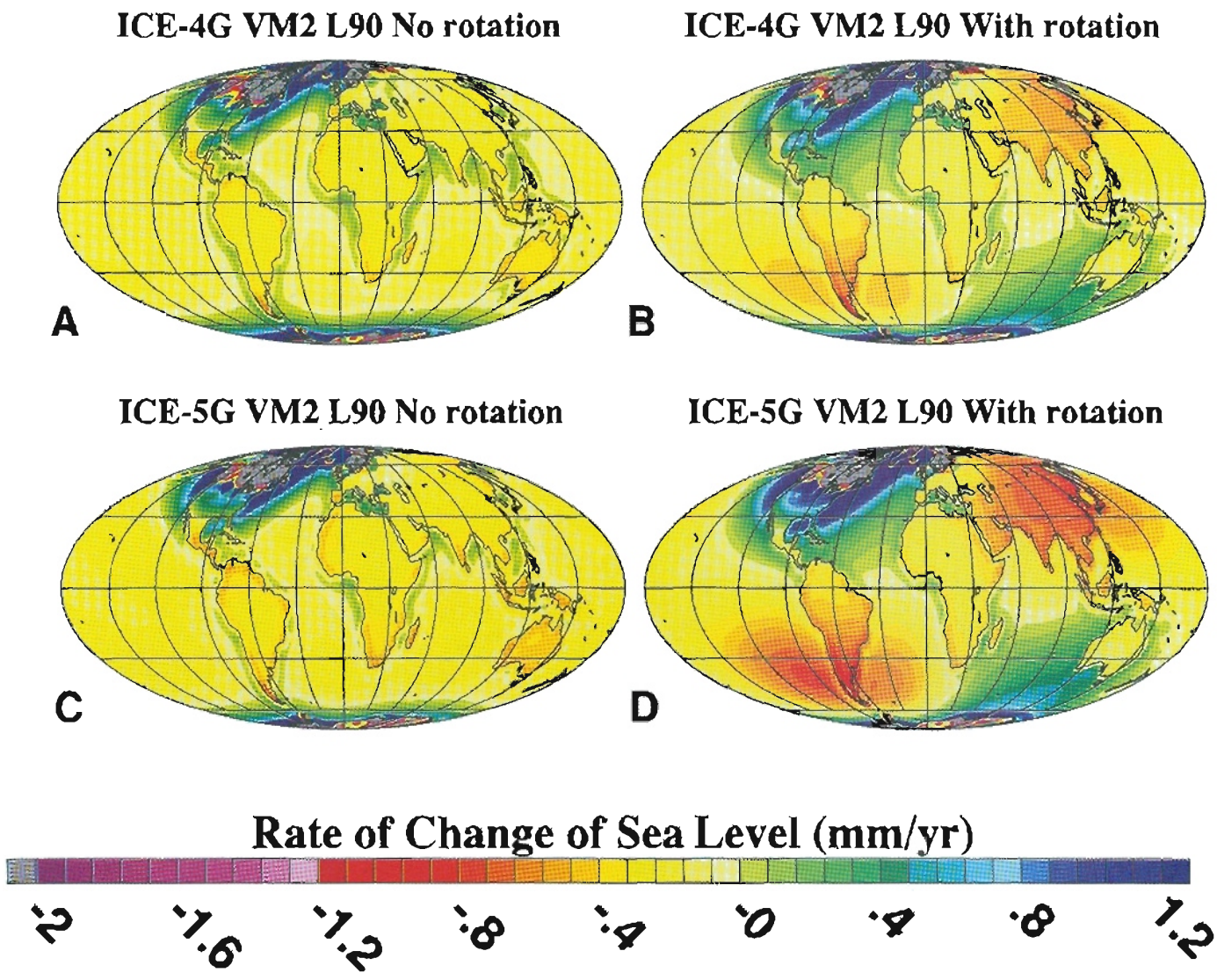

Figure 6. Global Mollweide projections of the present-day rate of relative sea-level rise for both the ICE-4G(VM2) and the ICE-5G(VM2) models of the glacial isostatic adjustment process. (A–B) Results for the ICE-4G(VM2) model, without and with the influence of rotational feedback included, respectively. (C–D) Results for the ICE-5G(VM2) model. Comparison of these results demonstrates that the influence of rotational feedback is stronger in the latter model than in the former, a consequence of the fact that the polar wander speed is predicted to be greater in the ICE-5G(VM2) model.

The most-important region for which reliable rotational feedback analyses may be performed is in the vicinity of the southern tip of the South American continent. Figure 8 shows a map of this continent, from which, along its east coast passive continental margin, radiocarbon-dated relative sea-level histories are available from each of the locations indicated. These data are especially important because they provide a traverse from the north coast of Venezuela, north of the equator, across the equator through Brazil to Argentina, ending finally along the southern Patagonian coast of Argentina and continuing to Terra del Fuego, the center of one of the four extrema that define the degree 2 and order 1 pattern. Comparison of this set of locations with the "quadrapolar" pattern of the rotational feedback effect on Figure 7 shows that this set of sites provides a traverse from the northernmost locations at which the feedback effect is expected to be small or absent to the southernmost sites where it is expected to be maximum.

Figures 9A and 9B show intercomparisons between the observed and predicted sea-level histories at 16 sites along this coast, all of the data from which were compiled and discussed in the paper by Rostami et al. (2000). On each fame of this set of intercomparisons, three different theoretical predictions are superimposed, one for the ICE-4G(VM2) model that includes the influence of rotational feedback (denoted "pr" in the model designations beneath the frames containing the individual intercomparisons; "p" for prehistory, indicating that a full glacial cycle has been employed in the calculation and "r" indicating that

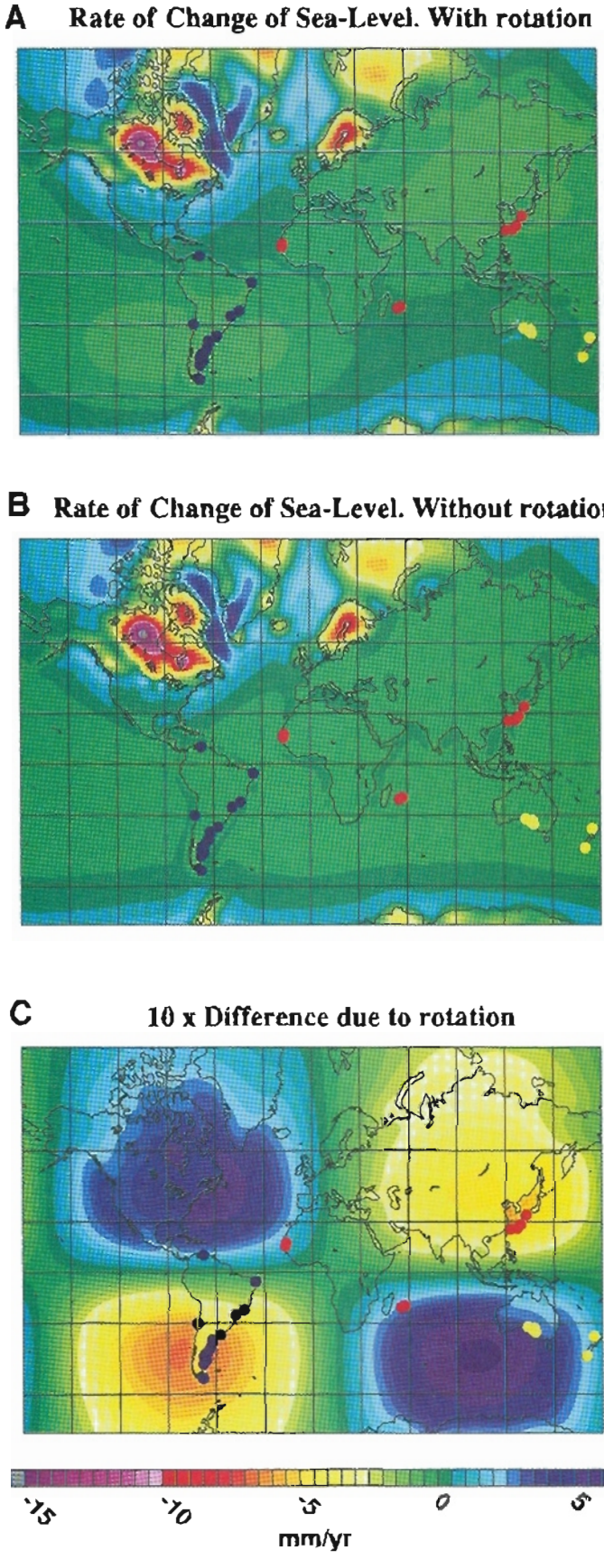

Figure 7. (A) Mercator projection of the present-day predicted rate of relative sea-level rise for the ICE-5G(VM2) model including the influence of rotational feedback. (B) Same as A but excluding the influence of rotational feedback. (C) The difference between A and B. Superimposed upon each of these maps are the locations of each of the sites at which intercomparisons between theory and observations are shown on Figures 9–11 for models that both include and exclude the influence of rotational feedback.

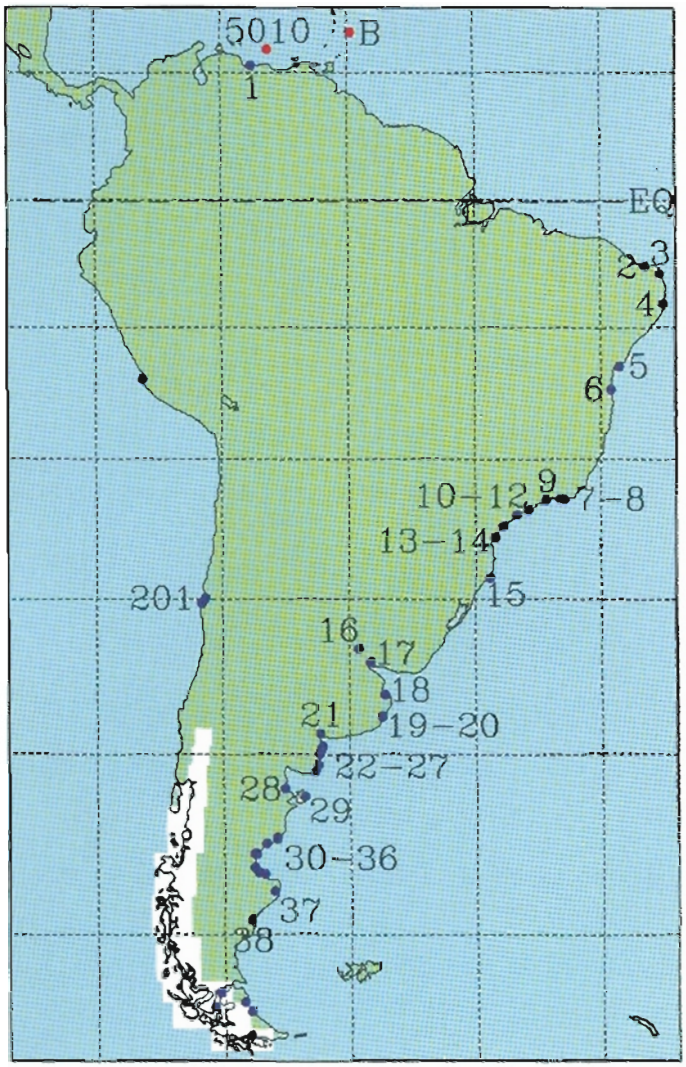

Figure 8. Location map for the sites along the east coast passive continental margin of the South American continent from which relative sea-level data may be employed to confirm the global theory of the glacial isostatic adjustment process. The site numbers correspond to the final two digits of the site numbers for which references are provided in Table 1. EQ—equator.

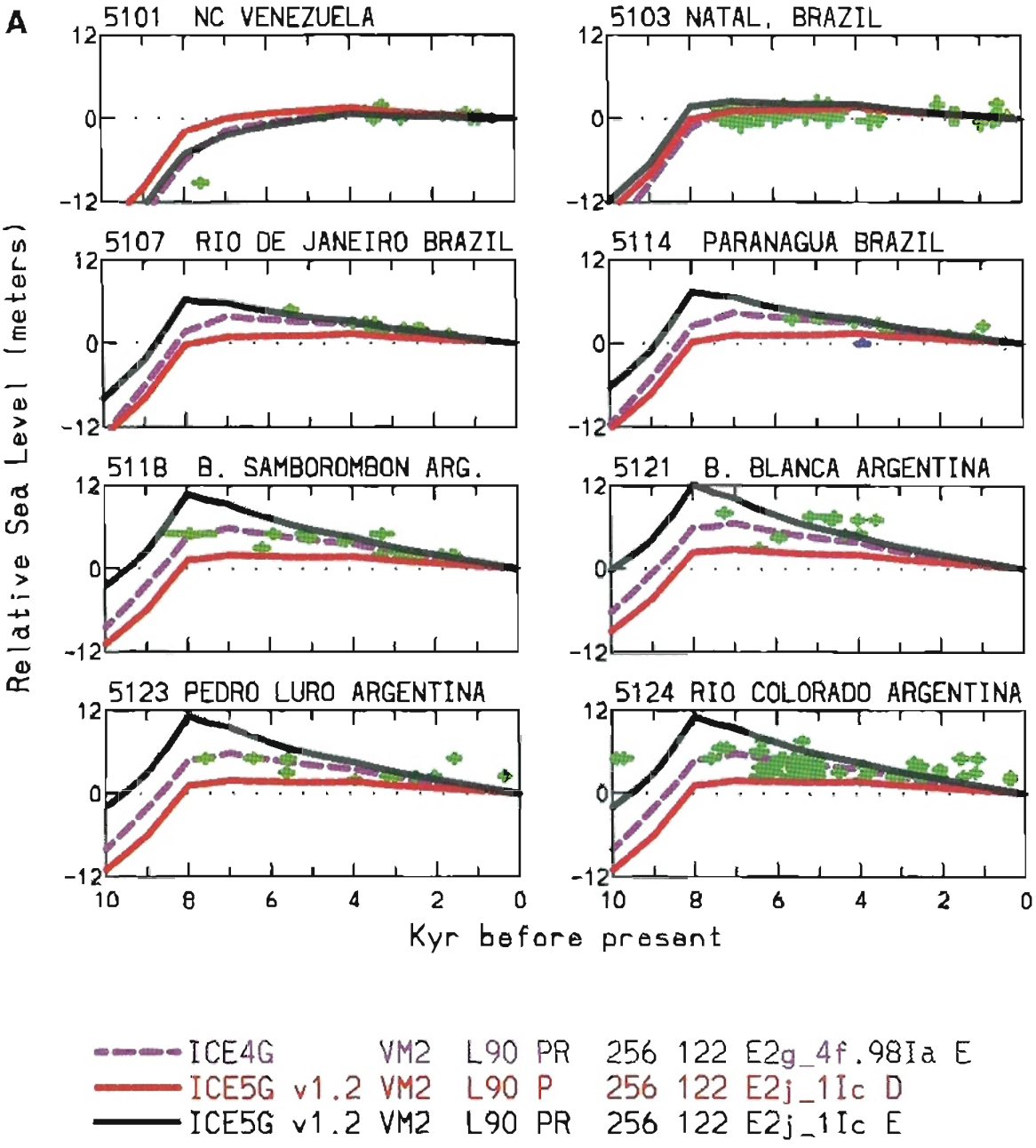

Figure 9 (*on this and following page*). (A) Comparisons between theory and observations at eight sites for which locations along the northern portion of the east coast of the South American continent are shown on Figure 8. The color-coded model designations at the bottom of the figure identify the theoretical predictions on each plate as belonging to either the ICE-4G(VM2) model with rotational feedback, the ICE-5G(VM2) model with rotational feedback (both models being designated "pr"), or the ICE-5G(VM2) model without rotational feedback (denoted simply "p," for prehistory, implying that the influence of a full glacial cycle has been included in the calculation but rotational feedback [denoted "r"] has not).

the influence of rotational feedback has also been included), and two for the ICE-5G(VM2) model, one of which includes the feedback effect and one of which excludes this influence. All of these calculations include the influence of a complete glacial-interglacial cycle. The importance of including the prediction for the ICE-4G(VM2) model with feedback in this set of intercomparisons lies in the fact that the influence of rotational feedback in this model is slightly weaker than it is in the ICE-5G(VM2) model as a consequence of the significant redistribution of the surface ice load in the most recent reconstruction. This redistribution of mass leads to a diminution in the predicted speed of true polar wander of ~20% and thus to a

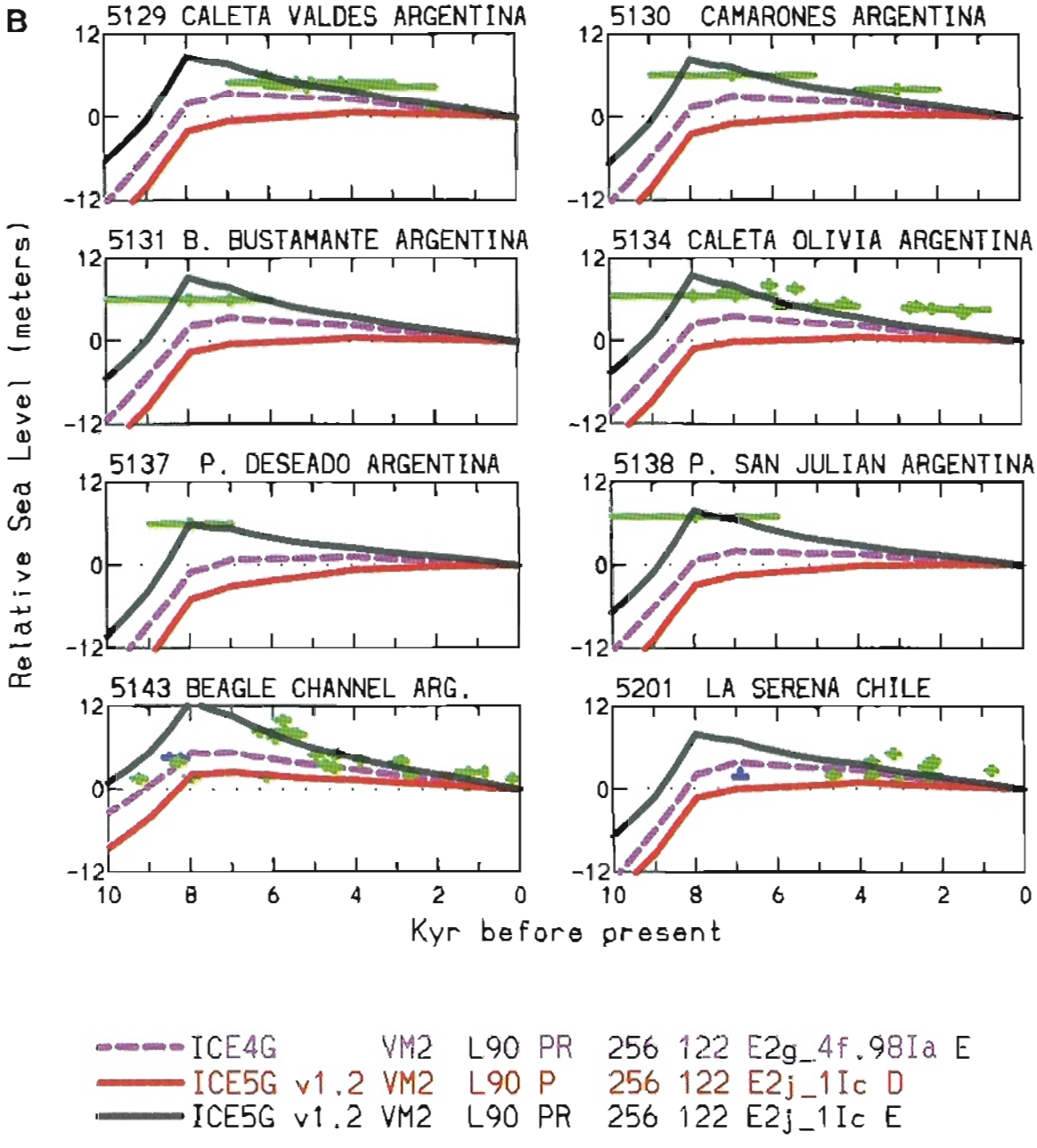

Figure 9 (*continued*). (B) Comparisons between theory and observations at eight additional sites for which locations along the southern portion of the east coast passive continental margin of the South American continent are shown on Figure 8. The color coding of the results for the different models is the same as in A.

weakening of the feedback onto sea-level history in this model compared to that in the ICE-5G(VM2) model.

Careful inspection of the set of intercomparisons shown on Figures 9A and 9B will establish a number of important facts (the sources for all of the additional data employed for the purpose of intercomparing theory and observations in this paper are listed on Table 1). First, it is clear that between the site on the north coast of Venezuela and the northernmost site from coastal Brazil, there is a change in the sign of the effect due to rotational feedback. At the Venezuelan site, which is north of the equator, the impact of this influence is to depress the predicted Holocene levels below those predicted in the absence of this feedback. At the northernmost

TABLE 1. REFERENCES FOR THIS PAPER'S DATA-MODEL INTERCOMPARISONS

Site no.	Site name	References
5101	NC Venezuela	Valastro et al. (1980)
5103	Natal, Brazil	Bezerra et al. (2003)
5107	Rio de Janeiro, Brazil	Martin et al. (1987); Fairbridge (1976); Delibrias et al. (1974); Angulo and Lessa (1997)
5114	Paranagua, Brazil	Angulo and Lessa (1997)
5118	B. Samborombon, Argentina	Codignotto et al (1992)
5121	B. Blanca, Argentina	Codignotto et al. (1992)
5123	Pedro Luro, Argentina	Albero and Angiolini (1983, 1985)
5124	Rio Colorado, Argentina	Codignotto et al. (1992)
5129	Caleta Valdes, Argentina	Rostami et al. (2000); Codignotto et al. (1992); Albero and Angiolini (1983)
5130	Camarones, Argentina	Rostami et al. (2000)
5131	B. Bustamante, Argentina	Rostami et al. (2000)
5134	Caleta Olivia, Argentina	Rostami et al. (2000)
5137	P. Deseado, Argentina	Rostami et al. (2000)
5138	P San Julian, Argentina	Rostami et al. (2000)
5143	Beagle Channel, Argentina	Porter et al. (1984); Morner (1991)
11105	Port Adelaide/Gillman, Australia	Belperio et al. (2002)
11107	Port Wakefield, Australia	Belperio et al (2002)
11109	Port Pirie (Spencer Gulf), Australia	Belperio et al. (2002)
11110	Redcliffe, Australia	Belperio et al. (2002)
11111	Franklin HB, Australia	Belperio et al. (2002)
11113	Ceduna, Australia	Belperio et al. (2002)
11115	Weiti River, New Zealand	Gibb (1986), Schofield (1975)
111123	Blue Skin Bay, New Zealand	Gibb (1986)
9003	Nouakchott, Mauritania	Faure and Hebrard (1977)
9006	St. Louis, Senegal	Faure et al. (980)
9022	Reunion	Camoin et al. (1977, 2004)
9023	Mauritius	Camoin et al. (1997)
11004	Shikoku Island, Japan	Pirazzoli (1978)
11006	Kikai-Jima Island, Japan	Pirazzoli (1978); Sugihara et al. (2003)
11008	S. Okinawa Island, Japan	Koba et al. (1982)
11010	Uotsuri Island, Japan	Koba et al. (1982)

Note: The site numbers for the named locations are those employed in the University of Toronto database of radiocarbon-dated relative sea-level histories.

Brazilian site however, the sign of the effect is opposite, and the influence of rotational feedback is to elevate predicted Holocene levels above those predicted in the absence of this influence. This change in sign of the feedback effect as the equator is crossed is exactly as expected on the basis of Figure 7. Moving ever further southward along the coast of Brazil toward Argentina the same hierarchy is maintained among the three different theoretical predictions. The highest level reached by the predicted mid-Holocene sea-level highstand is delivered by the version of the ICE-5G(VM2) model that includes feedback. The next highest level of this feature is predicted by the ICE-4G(VM2) model with feedback. The version of the ICE-5G(VM2) model that excludes the influence of rotational feedback always predicts the lowest amplitude of this feature, if any such feature is predicted to exist at all. Because of the scatter in the data sets shown on Figure 9A, it is often not possible to discriminate between the ICE-5G(VM2) and ICE-4G(VM2) predictions insofar as the quality of their fits to the data is concerned. However, it is abundantly clear that the feedback is absolutely required if the observed highstand amplitudes are to be understood at all. It is important to note that most of these data sets are from the older literature.

The comparisons shown on Figure 9B are much more definitive than those shown on Figure 9A, insofar as their ability to discriminate between the viability of the two models that include the feedback effect is concerned. All of the data shown on this figure were collected in the context of the doctoral dissertation of Kia Rostami and published in Rostami et al. (2000). Considerable effort was expended to ensure the accuracy of the inferences of relative sea level, as the amplitudes of the mid-Holocene highstands observed along this segment of the coast were found to be among the highest observed anywhere in the world. In Rostami et al. (2000), attention was also drawn to the fact that the amplitude of this characteristic feature appeared to increase systematically southward along the coast from northern Brazil to southern Argentina. The intercomparisons presented between the predictions of the ICE-4G(VM2) model without rotational feedback have demonstrated that this characteristic of the observations could not be understood in terms of the model. In Peltier (2002c), it was shown that proper incorporation of the influence of rotational feedback in the ICE-4G(VM2) model helped considerably to remove the residual misfits, although the highest-amplitude mid-Holocene highstand features remained imperfectly explained. This conclusion was reinforced in Peltier (2005), wherein it was suggested that the results could indicate that the theoretical model was accurately predicting the speed of polar wander driven by the glacial isostatic adjustment process. Inspection of the results shown on Figure 9B demonstrates that the residual misfits that remain between the predictions of the ICE-4G(VM2) model and the observations are entirely removed by the ICE-5G(VM2) version of the model, a version in which the predicted speed of true polar wander that controls the strength of the feedback is somewhat increased above that predicted by the ICE-4G(VM2) version.

Although it is extremely satisfying to have discovered the source of the remaining "signal" in the coastal records of Holocene relative sea-level history from the east coast passive continental margin of the South American continent, there clearly remains an issue as to whether data sets from the other three extrema of the spherical harmonic degree 2 and order 1 pattern might be invoked to confirm the uniqueness of this interpretation. To this end, consider first the additional set of intercomparisons shown on Figure 10, all of which concern sites at which the history of postglacial relative sea-level change is expected to be under the influence of the second Southern Hemisphere extremum of the rotational feedback effect. The first six of these sites

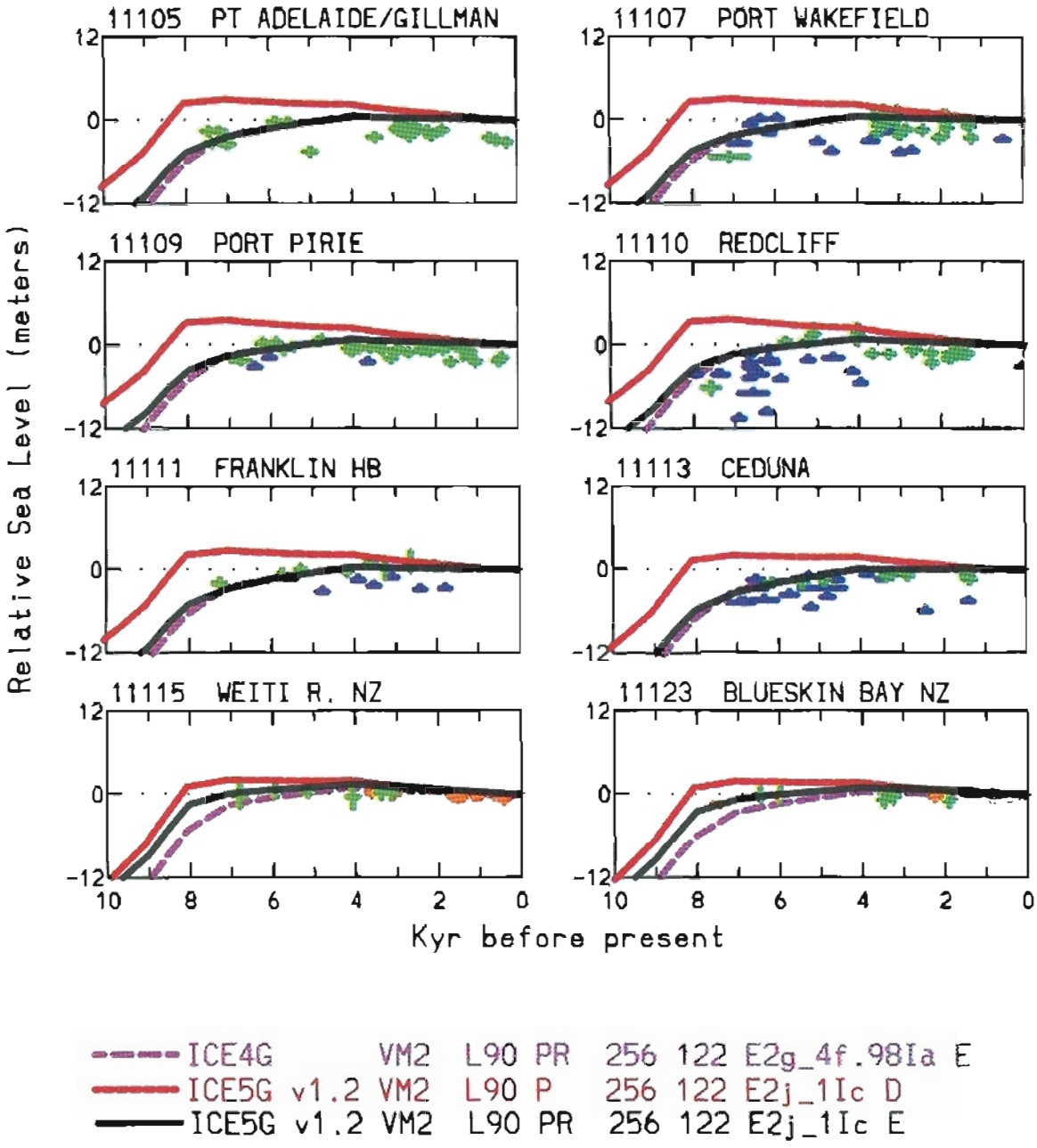

Figure 10. Comparisons between theory and relative sea-level observations at eight locations from southern Australia and New Zealand. These are sites at which the local relative sea-level history is under the influence of the second Southern Hemisphere extremum of the spherical harmonic degree 2 and order 1 pattern that is superimposed upon the predictions of postglacial relative sea-level history by the action of rotational feedback. The color coding of the results for the different models is the same as in 9A.

are located along the coast of southern Australia in the Great Australian Bight. The final two locations are from New Zealand. Based upon an inspection of Figure 7, it is clear that the sign of the rotational feedback effect is expected to be opposite to that at the South American locations. Inspection of the observations from these additional locations reveals that, whereas the data from the sites along the east coast of South America were characterized by large-amplitude mid-Holocene sea-level highstands, no such feature is evident at these additional eight locations. Inspection of the intercomparisons of the theoretical predictions for the same three versions of the theory employed in the analyses shown on Figures 9A and 9B demonstrates that,

in the absence of the influence of rotational feedback, the theory would predict a significant highstand amplitude at each of these locations. No such feature is observed. When this influence is added to the theory, however, the highstand is suppressed, and the theoretical predictions very accurately fit the relative sea-level observations at every location. This too, is a highly satisfying result, and it confirms the inference based upon the analysis of the South American data set. The speed of polar wander predicted by the ICE-5G(VM2) model, the characteristic of the model that enables it to fit the South American data set, is the same as that required to allow the model to fit the data from the South Pacific Ocean sector of the climate system, even though the data from this additional region are only marginally able to discriminate between the ICE-4G and ICE-5G versions of the model. This is almost certainly a consequence of the fact that the sites of the data are not sufficiently close to the maximum of the South Pacific extremum in the pattern of rotational feedback influence. The interpretation of the combined data set from South America and from the South Pacific Ocean therefore appears to be unique. Rotational feedback is exerting a controlling influence upon the Holocene records at these locations.

It is worth pointing out here that in the absence of recognition of the importance of rotational feedback, one might have been inclined to draw erroneous conclusions on the basis of relative sea-level observations such as those from the Great Australia Bight shown on Figure 10. One might, for example, be inclined to conclude that such data should be interpreted as evidence that global sea level continued to rise throughout the Holocene interval of time. This would be a "logical" error to make if one were employing a version of the theory of Peltier (1974; and subsequently, as recently reviewed in Peltier, 1998a) from which the influence of rotational feedback was excluded. One would then predict the existence of a mid-Holocene sea-level highstand at these sites unless one were to continue to add water to the global ocean from mid-Holocene time onward. Only in this way could one prevent the highstand from forming. Returning to a further examination of Figures 2 and 3, on which are superimposed the two versions of the eustatic sea-level curve of the ICE-5G model, it can be noted that these models are characterized by the fact that all continental ice-sheet melting is posited in them to have ceased by 4 ka. In spite of the fact that no water is being added to the ocean from 4 ka onward, the predicted relative sea-level histories at the sites in Australia and New Zealand that include the influence of rotational feedback are characterized by rising sea levels through this interval of time. This is entirely due to the influence of rotational feedback and has nothing to do with the continued addition of water to the global ocean.

An additional interesting issue has recently been raised in Mitrovica et al. (2005) who have suggested that the strength of the contribution of rotational feedback to one particular observable related to the glacial isostatic adjustment process may be inaccurately predicted by the theory of Peltier (1982) and Wu and Peltier (1984). This concerns the magnitude of the polar wander speed that is predicted by the theory and in particular the impact that this prediction makes upon the degree 2 and order 1 contribution to the time dependence of geoide height. However, their suggested modification of this theory has no impact upon the influence that rotational feedback has upon relative sea level history as these observations are being analyzed in this paper. The ICE-5G(VM2) model very nicely fits the observed speed and direction of true polar wander recorded in the International Latitude Service (ILS) data set of Vincente and Yumi (1969, 1970) when the original form of the theory of the rotational response to the GIA process is employed. Furthermore the claim in Mitrovica et al. (2005) that the original theory of Peltier (1982) and Wu and Peltier (1984) is based upon a mathematically unstable formulation is entirely erroneous and apparently based upon a lack of understanding of the Tauberian theorems.

A further and final set of intercomparisons between theory and observations from relative sea-level sites in the far field of the ice sheets is shown on Figure 11, where examples are shown from sites at which on the basis of Figure 7, one expects the mid-Holocene highstand to be suppressed, as well as from sites at which one expects this feature to be enhanced by the influence of rotational feedback. Locations of the former kind include sites in the Indian Ocean (under the influence of the same "bull's-eye" as that which controls the southern Australian data) and sites on the west coast of Africa (which are under the control of the "bull's-eye" that has its maximum off the east coast of the North American continent). Sites of the latter kind include those from the islands of Japan, where sea-level history is controlled by the fourth maximum of the spherical harmonic degree 2 and order 1 pattern. At these locations, one expects the influence of rotational feedback to contribute significantly to the development of a mid-Holocene highstand of the sea. Inspection of the set of intercomparisons in Figure 11 demonstrates that, at each one of the locations from which data are shown, expectations based upon theoretical understanding of the influence of rotational feedback are fully verified. At the Japanese island locations, in particular, the observed highstands are not understandable except as a consequence of the action of rotational feedback. Although these data are only marginally able to differentiate between the ICE-4G(VM2) and ICE-5G(VM2) models, they are entirely unambiguous in their requirement that the influence of rotational feedback be properly included in the calculation.

SUMMARY AND CONCLUSIONS

The two issues addressed in this paper, (1) the depth of the "ice-equivalent" eustatic sea-level lowstand during the LGM, and (2) the magnitude of the influence of rotational feedback upon postglacial relative sea-level history, have both been cause of debate in the recent literature. These issues are clearly very strongly linked. This can be understood on the basis of the fact that the greater the amount of ice involved in the glaciation-deglaciation cycle, the stronger the rotational response elicited by the glacial isostatic adjustment process and the more visible the influence of rotational feedback upon postglacial relative sea-level history. It is therefore crucial for an accurate assessment of

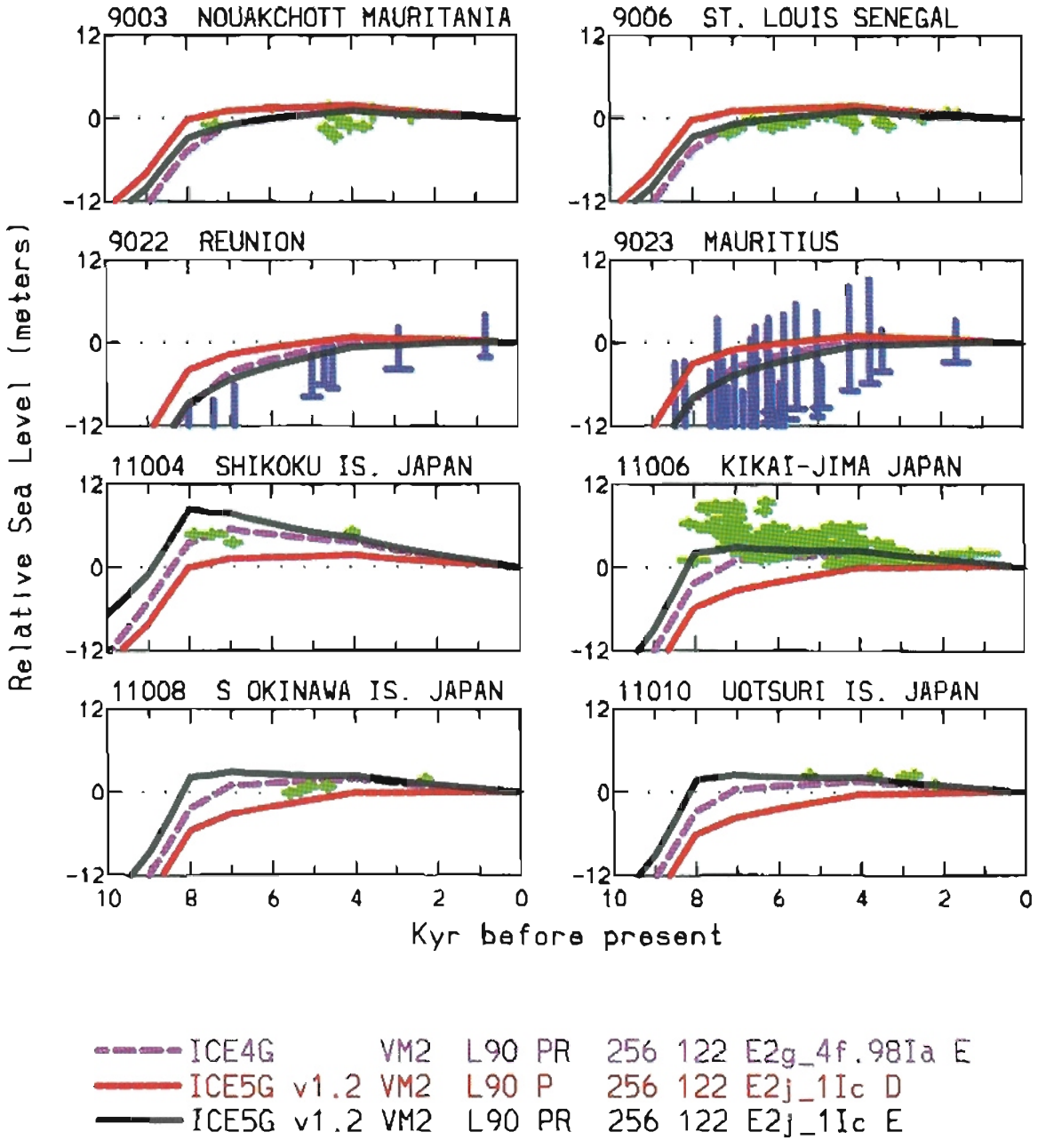

Figure 11. Comparisons between theory and relative sea-level observations at eight additional locations from the three extrema beyond the South American sector within which the influence of rotational feedback is strongest. The color coding of the results for the different models is the same as in 9A.

the importance of the latter influence to have knowledge of the amount of ice that was melted from the surface of the continents during the deglaciation process as well as the timing of this event. The importance of the extended relative sea-level record from the island of Barbados recently described in Peltier and Fairbanks (2006) is that it provides the most accurate available record with which to constrain both timing and amount. The discussion of the interpretation of this record provided herein adds to that in Peltier and Fairbanks (2006) by explicitly demonstrating the degree to which the predicted relative sea-level history at Barbados provides an accurate measurement of "ice-equivalent" eustatic sea-level history. As first pointed out in Peltier (2002a) in connection with a discussion of the ICE-4G(VM2) model, the actual coral-based record of sea-level history from Barbados provides a very good approximation to the "ice-equivalent" eustatic history. It makes this record especially valuable. The extended ver-

sion of this record, discussed in Peltier and Fairbanks (2006), has been shown to rule out the possibility of the existence of the large meltwater pulse that was hypothesized to have occurred at 19 ka by Yokoyama et al. (2000). It furthermore constrains the depth of the ice-equivalent eustatic lowstand to a value very close to the value of 120 m conventionally assumed (e.g., Shackleton, 2000). A corollary to this is the refutation of the claim in Lambeck and Chappell (2001) that there existed too little ice in the Northern Hemisphere at the LGM to explain the rise of sea level from the LGM onward. The ICE-5G model is characterized by an amount of melting emanating from the Antarctic continent that is in full accord with the results of a priori reconstructions based upon the application of glaciological models (e.g., Huybrechts, 2002; Denton and Hughes, 2002). The amount of ice contained in the glaciated regions of the Northern Hemisphere is strongly constrained by both local geomorphological and geodetic observations (see, e.g., Peltier, 2002c). Although the timing of the loss of mass from the northern hemisphere is very well constrained by the carbon-dated retreat isochrones, it is only recently (e.g., Domack et al., 2005; Leventer et al., 2006) that chronological control on the southern hemisphere retreat of the glaciation has become available. These data have established that southern hemisphere retreat occurred synchronously with the meltwater pulse 1b event that is clearly recorded in the extended Barbados record of Peltier and Fairbanks (2006). This timing of southern hemisphere retreat has always been assumed in the ICE-3G, ICE-4G, and ICE-5G sequence of models based upon other arguments.

Concerning the issue of the importance of the role that rotational feedback plays in controlling the detailed history of Holocene sea-level variability, the results discussed in this paper firmly establish that this influence is critical to the understanding of observed records from a variety of different geographical regions. The effect is strongest near the centers of the four extrema of the spherical harmonic degree 2 and order 1 pattern that arises due to the dominant role in the rotational feedback effect due to the polar wander component of the rotational response to the ice-age cycle. Through the analyses discussed in this paper, it has been firmly established that this influence is most apparent through the control that it exerts upon the height (and existence) of the mid-Holocene highstands of the sea in every geographical region in which the influence of such feedback is expected to be strong.

Although the theory that has been developed to explain the detailed characteristics of the global process of glacial isostatic adjustment has been rather successful, there do remain a number of issues to which attention must turn in future. Among these is the question of the accuracy of the VM2 profile of mantle viscosity and the extent to which it may be possible to further exploit the observables related to the glacial isostatic adjustment process in order to infer the nature of the lateral heterogeneity of this parameter that must exist in the mantle of Earth as well as the lateral variations in lithospheric thickness. As demonstrated in Peltier and Jiang (1996) and further discussed in Peltier (1998a), the viscosity of the deepest part of the lower mantle in the VM2 radial profile is constrained only by Earth rotation constraints of polar wander speed and nontidal acceleration of rotation. Since it is clear, based upon inferences of the globally averaged rate of sea-level rise over the past century, that both small ice sheets and glaciers (e.g., Meier, 1984; Dyurgerov and Meier, 2005), as well as the great polar ice sheets themselves (e.g., Krabill et al., 2000), must be contributing to the required addition of mass to the global oceans, and since this loss of continental ice will also influence the rotational observables, these observables will be contaminated by this effect due to greenhouse gas–induced global warming. The formal Bayesian inversions of the glacial isostatic adjustment data that delivered the VM2 profile, as discussed in detail in Peltier (1998b) were based upon the use of only the nontidal acceleration of rotation. There, and in related papers, it was shown that when this observable was "decontaminated" by subtracting the fraction of the observed signal that would be caused by a given and plausible assumed rate of polar ice-sheet melting, the modification to the mantle viscosity profile delivered by the Bayesian inversion consisted of an enhancement of the viscosity in the lower half of the lower mantle. Otherwise, the inferred profile was unaffected. With the launch of the Gravity Recovery and Climate Experiment (GRACE) dual satellite system, which is currently measuring the time dependence of the gravitational field of the planet, it will soon be possible to more accurately measure the ongoing rates of polar ice-sheet and glacier melting, and this will lead to much improved constraints upon the mantle viscosity profile. In the interpretation of the GRACE observations, it will be critical to have accurate predictions of the time dependence of geoid height that is expected due to the action of the glacial isostatic adjustment effect associated with the late Pleistocene ice-age cycle. Figure 12 compares the prediction of this field for the ICE-5G(VM2) version 1.3 model with the GRACE observations for the North American continental region of heaviest LGM ice cover. Both the GIA prediction and the GRACE observations are represented in terms of the time rate of change of the gravitationally equivalent thickness of a layer of water at the surface of Earth. The fact that the ICE-5G(VM2) prediction rather accurately matches the GRACE observation constitutes an important further validation of the quality of this model. Notable on the plot of the residual signal that remains when the GIA prediction is subtracted from the GRACE observations are the regions of high rates of mass loss over both Greenland and the high topography regions of the U.S. State of Alaska and the Yukon Territory of Canada. The signals over these regions are due to the ongoing rates of disintegration of land ice that is occurring, most probably, as a consequence of the impact of high latitude global warming. Over Greenland the observed signal is such as to represent a contribution to global sea-level rise that is on the order of 0.5 mm/yr, a highly significant fraction of the approximately 2.8 mm/yr of rise that has been inferred on the basis of TOPEX/POSEIDON satellite altimetric measurements.

Insofar as glacial isostatic adjustment–related observations can be used to constrain the lateral variations in mantle viscosity, there currently do not exist misfits of the spherically symmetric

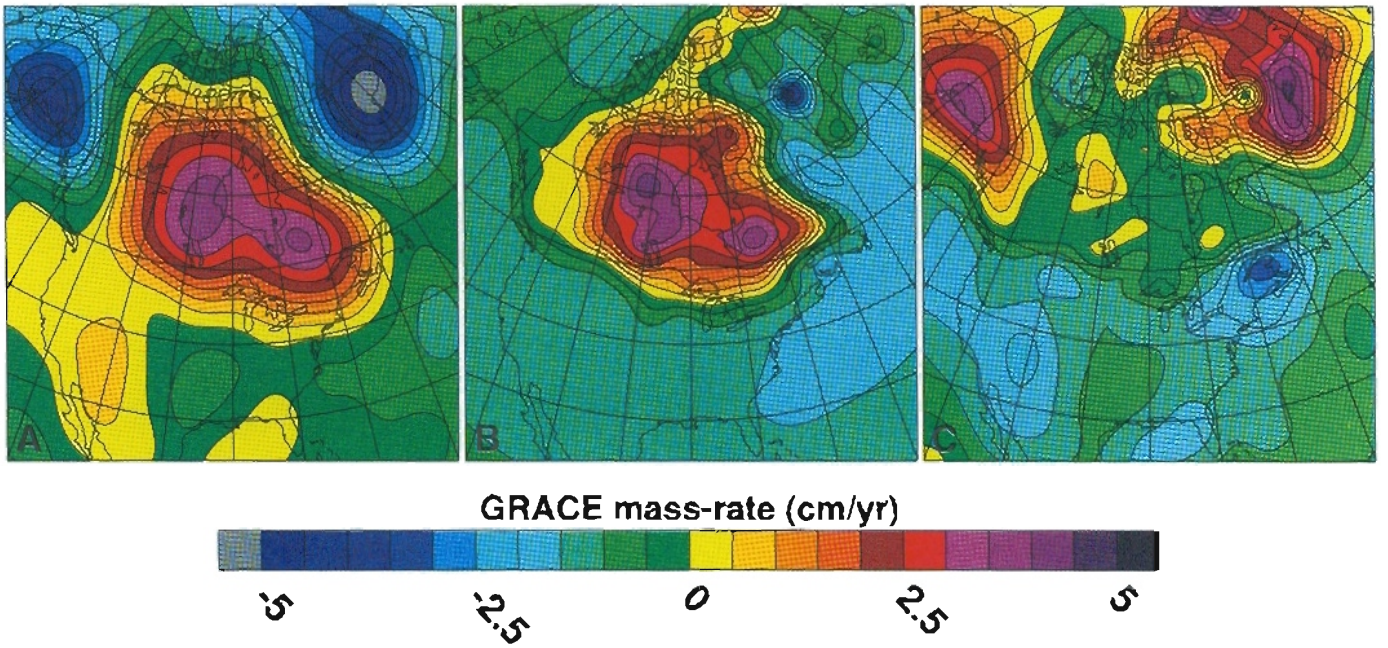

Figure 12. This shows an inter-comparison between the GRACE observations of the time rate of change of the gravitational field over the North American continent shown in (A) and the prediction of the ICE-5G model of Peltier (2004) in (B). The difference between these two fields is shown in (C). The representation of the gravitational field shown is in terms of the time rate of change of the thickness of an equivalent layer of water at Earth's surface which is referred to in the label on the color bar as "mass rate" and which has the dimensions of cm/yr. For the purpose of this inter-comparison, the depth dependence of the viscosity of the mantle has been taken to be equal to the VM3 model of Peltier (1998a) which differs from the VM2 model only in the viscosity of the deepest part of the lower mantle. This adjustment of the viscosity profile is required in order to account for the contribution to the non-tidal acceleration in the rate of planetary rotation that results from the high rate of melting that is currently occurring on both Greenland and the high mountains of Alaska and the Yukon Territory. That such melting is currently ongoing is shown by the high rates of decreasing equivalent water layer thickness evident in the GRACE data over these regions.

models to the observations that one would necessarily be obliged to map into inferred lateral variations in this parameter, except in those regions such as Iceland or the Basin and Range geological province of the western United States, which are known to be thermally anomalous. The success of the ICE-5G(VM2) model from a global perspective is highly suggestive that the lateral heterogeneity of viscosity that must exist in a medium like the mantle of Earth, which is undergoing vigorous thermal convection, is confined to regions of such modest horizontal scale that its influence upon the global process may be very difficult to discern. Nevertheless, work is proceeding to develop models of the glacial isostatic adjustment phenomenon that include the influence of the lateral heterogeneity of viscosity, and these may eventually prove useful in further advancing our understanding of the system within which the process is occurring (see, e.g., the papers by Wu and others in the book edited by Patrick Wu [1998], as well as the more recent contributions from his group).

One further issue that is worth emphasizing here concerns the important role that the theory of the glacial isostatic adjustment process continues to play in the climatologically important problem of reconstructing the global paleotopography and continental ice-cover distribution through the glacial cycle. As mentioned in the introduction to this paper, analyses performed with the theory continue to produce the standard models of the surface boundary conditions that are required in the application of modern coupled atmosphere-ocean general circulation models for the purpose of reconstructing past climate states. Very recently, the theory has been successfully coupled to a full three-dimensional thermomechanical model of continental ice-sheet evolution, and this has been employed to compute detailed meltwater run-off histories from the continents (e.g., Tarasov and Peltier, 2004, 2005, 2006). The University of Toronto Glacial Systems Model has enabled the validation of what appears to be the correct explanation for the Younger Dryas cold episode, which interrupted the Northern Hemisphere climate warming that was associated with the most recent glacial-interglacial transition. Although it had previously been thought that this event was caused by a switch in the direction of Laurentide (North American) ice-sheet derived continental run-off from the south through the Mississippi outlet to the east through the Gulf of St. Lawrence, analyses using the University of Toronto Glacial Systems Model have suggested that the actual switch was from the south to the north through the McKenzie River outlet directly into the Arctic Ocean. This appears to have resolved an important issue in the understanding of the specific variations of Northern Hemisphere climate that accompanied the last deglaciation event. Recently discussed simulations of the

response of the Atlantic thermohaline circulation to such Arctic freshwater forcing (Peltier et al., 2006) demonstrate this to be an entirely viable explanation for the Y-D event.

This connection between the glacial isostatic adjustment phenomenon and hydrological processes is currently being extended to include subsurface as well as surface-water fluxes. The way in which the subsurface continental aquifer may have been recharged during the late Pleistocene glacial cycle is an extremely interesting question. The University of Toronto Glacial Systems Model is perfectly suited for this application, and early results from this work are highly suggestive that important insights will be forthcoming as the work proceeds. Results from this effort will be reported in due course.

ACKNOWLEDGMENTS

I am indebted to Claire Waelbroeck for providing me with the eustatic sea-level reconstructions from both Waelbroeck et al. (2002) and Lambeck and Chappell (2001). This work has been supported by both the Polar Climate Stability Network, which is funded by the Canadian Foundation for Climate and Atmospheric Science and a consortium of Canadian universities, and by Natural Sciences and Engineering Research Council Grant A9627.

REFERENCES CITED

Al-Asfour, T.A., 1982, Changing sea level along the north coast of Kuwait Bay: Boston, Kegan Paul International Ltd., 186 p. (Source of data for site KU on Figure 5.)

Albero, M.C., and Angiolini, F.F., 1983, INGEIS Radiocarbon Laboratory dates I: Radiocarbon, v. 25, p. 831–842.

Albero, M.C., and Angiolini, F.E., 1985, INGEIS Radiocarbon Laboratory dates II: Radiocarbon, v. 27, p. 315–337.

Angulo, R.J., and Lessa, G.C., 1997, Brazilian sea level curves: A critical review with emphasis on the curves from the Parangua and Cananeia regions: Geology, v. 140, p. 141–166.

Bard, E., Hamelin, B., Fairbanks, R.G., and Zindler, A., 1990, Calibration of the ^{14}C timescale over the past 30,000 years using mass spectrometric U-Th ages from Barbados corals: Nature, v. 345, p. 405–409, doi: 10.1038/345405a0.

Belperio, A.P., Harvey, N., and Bousman, R.P., 2002, Spatial and temporal variability in the Holocene sea-level record of the south Australian coastline: Sedimentary Geology, v. 150, p. 153–169, doi: 10.1016/S0037-0738(01)00273-1

Bezerra, I., Barreto, A., and Sugio, K., 2003, Holocene sea-level history on the Rio Grande do Norte State coast, Brazil: Marine Geology, v. 196, p. 73–89, doi: 10.1016/S0025-3227(03)00044-6.

Camoin, G.F., Colonna, M., Montaggioni, L.F., Casanova, J., Faure, G., and Thomassin, B.A., 1997, Holocene sea level changes and reef development in the southwestern Indian Ocean: Coral Reefs, v. 16, p. 247–259, doi: 10.1007/s003380050080.

Camoin, G.F., Montaggioni, L.F., and Braithwaite, C.J.R., 2004, Late glacial to postglacial sea levels in the western Indian Ocean: Marine Geology, v. 206, p. 119–146, doi: 10.1016/j.margeo.2004.02.003.

Cato, I., 1992, Shore displacement data based upon lake isolations confirm the postglacial part of the Swedish Geochronological Timescale: Sveriges Geologiska Undersokoning, ser. Ca 81, p. 75–80. (Source of data for site AN of Figure 5.)

Chappell, J., Omura, A., Esat, T., McCulloch, M., Pandelfi, J., Ota, Y., and Pillans, B., 1996, Reconciliation of Late Quaternary sea levels derived from coral terraces at Huon Peninsula with deep sea oxygen isotope records: Earth and Planetary Science Letters, v. 141, p. 227–236, doi: 10.1016/0012-821X(96)00062-3.

Clark, J.A., Farrell, W.E., and Peltier, W.R., 1978, Global changes in postglacial sea level: A numerical calculation: Quaternary Research, v. 9, p. 265–287, doi: 10.1016/0033-5894(78)90033-9.

Codignotto, J.D., Kokott, R.R., and Marcomini, S.C., 1992, Neotectonism and sea-level changes in the coastal zone of Argentina: Journal of Coastal Research, v. 8, p. 125–133.

Dahlen, F.A., 1976, The passive influence of the oceans on the rotation of the Earth: Geophysical Journal of the Royal Astronomical Society, v. 46, p. 363–406.

Denton, G.H., and Hughes, T., 2002, Reconstructing the Antarctic ice sheet at the Last Glacial Maximum: Quaternary Science Reviews, v. 21, p. 193–202, doi: 10.1016/S0277-3791(01)00090-7.

Dubar, J.R., and Anthony, E.J., 1995, Holocene environmental change and river mouth sedimentation in the Baie des Anges, French Riviera: Quaternary Research, v. 43, p. 329–343. (Source of data for site BA On Figure 5.)

Dyurgerov, M.B., and Meier, M.F., 2005, Glaciers and the changing earth system: A 2004 Snapshot, Occasional Paper No. 58, Institute of Arctic and Alpine Research: Boulder, Colorado, University of Colorado.

Fairbanks, R.G., 1989, A 17,000 year glacial eustatic sea level record: Influence of glacial melting rates on the Younger Dryas event and deep ocean circulation: Nature, v. 342, p. 637–641, doi: 10.1038/342637a0.

Fairbanks, R.G., Mortlock, R.A., Chiu, T.-C., Cao, L., Kaplan, A., Guildersen, T.P., Fairbanks, T.W., Bloom, A.L., Grootes, P.M., and Nadeau, M. J., 2005, Radiocarbon calibration curve spanning 0 to 50,000 years BP based on paired 230Th/234U/238U and 14C dates on pristine corals: Quaternary Science Reviews, v. 24, no. 16–17, p. 1781–1796, doi: 10.1016/j.quascirev.2005.04.007.

Farrell, W.E., and Clark, J.A., 1976, On postglacial sea level: Geophysical Journal of the Royal Astronomical Society, v. 46, p. 647–667.

Faure, H., and Hebrard, L., 1977, Variations des lignes de ravages au Senegal et au Mauritania au Cours de l'Holocene: Studia Geologica Polonica, v. 52, p. 143–157.

Faure, H., Fontes, J.C., Hebrard, L., Monteillet, J., and Pirazolli, P.A., 1980, Geoidal changes and shore level tilt along Holocene estuaries: Senegal River area, West Africa: Science, v. 210, p. 421–423, doi: 10.1126/science.210.4468.421

Gibb, J.G., 1986, A New Zealand regional Holocene eustatic sea-level curve and its application to determination of vertical tectonic movements: Royal Society of New Zealand Bulletin, v. 24, p. 377–395.

Hall, B.L., and Denton, G.H., 1999, New relative sea level curves for the southern Scott Coast, Antarctica: Evidence for Holocene deglaciation of the western Ross Sea: Journal of Quaternary Science, v. 14, p. 641–650. (Source of data for site SC on Figure 5.)

Hanebuth, T., Statteger, K., and Grootes, P.M., 2000, Rapid flooding of the Sunda shelf: A late glacial sea level record: Science, v. 288, p. 1033–1035, doi: 10.1126/science.288.5468.1033.

Huybrechts, P., 2002, Sea level changes at the LGM from ice dynamic reconstructions of the Greenland and Antarctic ice sheets during the glacial cycles: Quaternary Science Reviews, v. 21, p. 203–231, doi: 10.1016/S0277-3791(01)00082-8.

Imbrie, J., Hays, J.D., Martinsen, D.G., McIntyre, A., Mix, A.C., Morley, J.J., Pisias, N.G., Prell, W.L., and Shackleton, N.J., 1984, The orbital theory of Pleistocene climate: Support from a revised chronology of the marine $\delta^{18}O$ record, *in* Berger, A., et al., Milankovitch and Climate: Norwell, Massachusetts, D. Reidel, p. 269–306.

Kaye, C.A., and Barghoorn, E., 1964, Late Quaternary sea level change and crustal rise in Boston, Massachusetts, with notes on the autocompaction of peat: Geological Society of America Bulletin, v. 75, p. 63–80. (Source of data for site BN on Figure 5.)

Koba, M., Nakata, T., and Takahashi, T., 1982, Late Holocene eustatic changes deduced from geomorphological features and their C-14 dates in the Ryuku Islands, Japan: Palaeogeography, Palaeoclimatology, Palaeoecology, v. 39, p. 231–260, doi: 10.1016/0031-0182(82)90024-4.

Krabill, W., Abdalati, W., Frederick, E., Manizade, F., Martin, C., Sonntag, J., Swift, R., Thomas, R., Wright, W., and Jungel, J., 2000, Greenland ice sheet: High elevation balance and peripheral thinning: Science, v. 289, p. 428–430, doi: 10.1126/science.289.5478.428.

Lambeck, K., and Chappell, J., 2001, Sea level changes through the last glacial cycle: Science, v. 292, p. 679–686, doi: 10.1126/science.1059549.

Leventer, A., Domack, E., Dunbar, R., Pike, J., Stickley, C., Maddison, E., Brachfield, S., Manley, P., and McClennan, C., 2006, Marine sediment

record from East Antarctica margin reveals dynamics of ice sheet recession: GSA Today, v. 16, no. 12, p. 4–10, doi: 10.1130/GSAT01612A.1.

Martin, L., Sugio, K., Flexor, J.M., Dominguez, J.M.L., and Bittencourt, A.C.S.P., 1987, Quaternary evolution of the central part of the Brazilian coast: The role of relative sea-level variation and of shoreline drift, *in* Quaternary Coastal Geology of West Africa and South America: United Nations Educational, Scientific and Cultural Organization Reports in Marine Science, v. 43, p. 97–145.

Meier, M., 1984, Contributions of small glaciers to global sea level: Science, v. 226, p. 1418–1421, doi: 10.1126/science.226.4681.1418.

Mitrovica, J.X., Wahr, J., Matsuyama, I., and Paulson, A., 2005, The rotational stability of an ice-age Earth: Geophysical Journal International, v. 161, p. 491–506, doi: 10.1111/j.1365-246X.2005.02609.x.

Morner, N.-A., 1991, Holocene sea level changes in the Terra del Fuego region: Bol. IG-USP: Publ. Esp., v. 8, p. 133–151.

Peltier, W.R., 1974, The impulse response of a Maxwell Earth: Reviews in Geophysics, v. 12, p. 649–669.

Peltier, W.R., 1976, Glacial isostatic adjustment. II: The inverse problem: Geophysical Journal of the Royal Astronomical Society, v. 46, p. 669–706.

Peltier, W.R., 1982, Dynamics of the ice age Earth: Advances in Geophysics, v. 24, p. 1–146.

Peltier, W.R., 1986, Deglaciation induced vertical motion of the North American continent and transient lower mantle rheology: Journal of Geophysical Research, v. 91, p. 9099–9123.

Peltier, W.R., 1994, Ice age paleotopography: Science, v. 265, p. 195–201, doi: 10.1126/science.265.5169.195.

Peltier, W.R., 1996, Mantle viscosity and ice age ice sheet topography: Science, v. 273, p. 1359–1364, doi: 10.1126/science.273.5280.1359.

Peltier, W.R., 1998a, Postglacial variations in the level of the sea: Implications for climate dynamics and solid Earth geophysics: Reviews in Geophysics, v. 36, p. 603–689, doi: 10.1029/98RG02638.

Peltier, W.R., 1998b, Implicit ice in the global theory of glacial isostatic adjustment: Geophysical Research Letters, v. 25, p. 3957–3960. (See also for data for site HB on Figure 5.)

Peltier, W.R., 1998c, The inverse problem for mantle viscosity: Inverse Problems v. 14, 441–478.

Peltier, W.R., 1999, Global sea level rise and glacial isostatic adjustment: Global and Planetary Change, v. 20, p. 93–123, doi: 10.1016/S0921-8181(98)00066-6.

Peltier, W.R., 2001, Global glacial isostatic adjustment and modern instrumental records of relative sea level history, in Douglas, B.C., Kearney, M.S., and Leatherman, S.R., eds., Sea Level Rise: History and Consequences: Academic Press, San Diego, p. 65–93.

Peltier, W.R., 2002a, On eustatic sea level history: Last Glacial Maximum to Holocene: Quaternary Science Reviews, v. 21, p. 377–396, doi: 10.1016/S0277-3791(01)00084-1.

Peltier, W.R., 2002b, Comments on the paper of Yokoyama et al. (2000) entitled "Timing of Last Glacial Maximum from observed sea level minima": Quaternary Science Reviews, v. 21, p. 409–414.

Peltier, W.R., 2002c, Global glacial isostatic adjustment: Paleo-geodetic and space geodetic tests of the ICE-4G(VM2) model: Journal of Quaternary Science, v. 17, p. 491–510, doi: 10.1002/jqs.713.

Peltier, W.R., 2004, Global glacial isostasy and the surface of the ice age Earth: The ICE-5G(VM2) model and GRACE: Annual Reviews in Earth and Planetary Science, v. 32, p. 111–149, doi: 10.1146/annurev.earth.32.082503.144359.

Peltier, W.R., 2005, On the hemispheric origins of meltwater pulse 1a: Quaternary Science Reviews, v. 24, p. 1655–1671, doi: 10.1016/j.quascirev.2004.06.023.

Peltier, W.R., and Andrews, J.T., 1976, Glacial isostatic adjustment. I: The forward problem: Geophysical Journal of the Royal Astronomical Society, v. 46, p. 605–646.

Peltier, W.R., and Drummond, R., 2002, A "broad shelf effect" in the global theory of postglacial relative sea level history: Geophysical Research Letters, v. 29, p. 1169, doi: 10.1029/2001GL014273.

Peltier, W.R., and Fairbanks, R.G., 2006, Global glacial ice volume and Last Glacial Maximum duration from an extended Barbados sea level record: Quaternary Science Reviews, v. 25, p. 3322–3337, doi: 10.1016/j.quascirev.2006.04.010.

Peltier, W.R., and Jiang, X., 1996, Mantle viscosity from the simultaneous inversion of multiple data sets pertaining to postglacial rebound: Geophysical Research Letters, v. 23, p. 503–506, doi: 10.1029/96GL00512.

Peltier, W.R., and Tushingham, A.M., 1989, Global sea level rise and the greenhouse effect: Might they be connected?: Science, v. 244, p. 806–810, doi: 10.1126/science.244.4906.806.

Peltier, W.R., Farrell, W.E., and Clark, J.A., 1978, Glacial isostasy and relative sea level: A global finite element model: Tectonophysics, v. 50, p. 81–110, doi: 10.1016/0040-1951(78)90129-4.

Peltier, W.R., Vettoretti, G., and Stastna, M., 2006, Atlantic meridional overturning and climate response to Arctic Ocean freshening: Geophysical Research Letters, v. 38, doi: 10.1029/2005GL025251.

Pickrill, R.A., 1976, Evolution of coastal landforms of the Wairau Valley: New Zealand Geographer, v. 32, p. 17–29. (Source of data for site WV on Figure 5.)

Pinot, S., Ramstein, G., Harrison, S.P., Prentice, I.C., Guiot, J., Stute, M., and Joussaume, S., 1999, Tropical paleoclimates at the Last Glacial Maximum: Comparison of Paleoclimate Modelling–Intercomparison Project (PMIP) simulations and paleodata: Climate Dynamics, v. 15, p. 857–874, doi: 10.1007/s003820050318.

Pirazzoli, P., 1978, High stands of Holocene sea levels in the NW Pacific: Quaternary Research, v. 10, p. 1–29, doi: 10.1016/0033-5894(78)90010-8.

Porter, S.C., Stuiver, M., and Heusser, C.J., 1984, Holocene sea-level changes along the Straits of Magellan and Beagle Channel, southernmost South America: Quaternary Research, v. 22, p. 59–67, doi: 10.1016/0033-5894(84)90006-1.

Rostami, K., Peltier, W.R., and Mangini, A., 2000, Quaternary marine terraces, sea level changes and uplift history of Patagonia, Argentina: Comparison with predictions of the ICE-4G (VM2) model of the global process of glacial isostatic adjustment: Quaternary Science Reviews, v. 19, p. 1495–1525, doi: 10.1016/S0277-3791(00)00075-5.

Schofield, J.C., 1975, Sea-level fluctuations cause periodic post-glacial progradation, South Kaipara Barrier, North Island, New Zealand: New Zealand Journal of Geology and Geophysics, v. 18, p. 295–316.

Shackleton, N.J., 2000, The 100,000 year ice age cycle identified and found to lag temperature, carbon dioxide, and orbital eccentricity: Science, v. 289, p. 1897–1902, doi: 10.1126/science.289.5486.1897.

Shennan, I., and Milne, G., 2003, Sea level observations around the Last Glacial Maximum from the Bonaparte Gulf, NW Australia: Quaternary Science Reviews, v. 22, p. 1543–1547, doi: 10.1016/S0277-3791(03)00088-X.

Shennan, I., Innes, J.B., Long, A.J., and Zong, Y., 1993, Late Devensian and Holocene relative sea level changes in northwest Scotland: New data to test existing models: Quaternary International, v. 26, p. 97–123. (Source of data for site AR on Figure 5.)

Siddall, M., Rohling, E.J., Almogi-Labin, A., Hemleben, Ch., Meischner, D., Schmelzer, I., and Smeed, D.A., 2003, Sea-level fluctuations during the last glacial cycle: Nature, v. 423, p. 853–858, doi: 10.1038/nature01690.

Siddall, M., Smeed, D.A., Hemleben, C., Rohling, E.J., Schmelzer, I., and Peltier, W.R., 2004, Understanding the Red Sea response to sea level: Earth and Planetary Science Letters, v. 225, p. 421–434, doi: 10.1016/j.epsl.2004.06.008.

Sugihara, K., Nakamori, T., Iryu, Y., Sasakai, K., and Blanchon, P., 2003, Holocene sea-level change and tectonic uplift deduced from raised reef terraces, Kikai-Jima, Ryuku Islands, Japan: Sedimentary Geology, v. 159, p. 5–25.

Tarasov, L., and Peltier, W.R., 2004, A geophysically constrained large ensemble analysis of the deglacial history of the North American ice sheet complex: Quaternary Science Reviews, v. 23, p. 359–388, doi: 10.1016/j.quascirev.2003.08.004.

Tarasov, L., and Peltier, W.R., 2005, Arctic forcing of the Younger Dryas cold reversal: Nature, v. 435, p. 662–665, doi: 10.1038/nature03617.

Tarasov, L., and Peltier, W.R., 2006, A calibrated deglacial chronology for the North American continent: Evidence of an Arctic trigger for the Younger Dryas event: Quaternary Science Reviews, v. 25, p. 659–688, doi: 10.1016/j.quascirev.2005.12.006.

Tushingham, A.M., and Peltier, W.R., 1991, ICE 3G: A new global model of Late Pleistocene deglaciation based upon geophysical predictions of postglacial relative sea level change: Journal of Geophysical Research, v. 96, p. 4497–4523.

Valastro, S., Davis, L.M., Vallrela, A.G., and Ekland-Olson, C., 1980, University of Texas at Austin radiocarbon dates XIV: Radiocarbon, v. 22, p. 1090–1115.

Vincente, R.O., and Yumi, S., 1969, Co-ordinates of the pole (1899–1968) returned to the conventional international origin: Publications of the International Latitude Observatory of Mizusawa, v. 7, p. 41–50.

Vincente, R.O., and Yumi, S., 1970, Revised values (1941–1961) of the co-ordinates of the pole referred to the CIO: Publications of the International Latitude Observatory of Mizusawa, v. 7, 109–112.

Waelbroeck, C., Labeyrie, L., Michel, E., Duplessy, J.-C., McManus, J., Lambeck, K., Balbon, E., and Labracherie, M., 2002, Sea-level and deep water temperature changes derived from benthic foraminifera isotopic records: Quaternary Science Reviews, v. 21, p. 295–305, doi: 10.1016/S0277-3791(01)00101-9

Wu, P., 1998, Dynamics of the Ice Age Earth: A Modern Perspective, Vol. 3–4: Ütikon-Zürich, Switzerland, Trans Tech Publications, 637 p.

Wu, P., and Peltier, W.R., 1984, Pleistocene deglaciation and the Earth's rotation: A new analysis: Geophysical Journal of the Royal Astronomical Society, v. 76, p. 202–242.

Yokoyama, Y., Lambeck, K., De Dekkar, P., Johnston, P., and Fifield, L.K., 2000, Timing of Last Glacial Maximum from observed sea level minima: Nature, v. 406, p. 713–716, doi: 10.1038/35021035.

Yokoyama, Y., Lambeck, K., De Dekkar, P., Johnston, P., and Fifield, L.K., 2001, Correction to Yokoyama et al. (2000): Nature, v. 412, p. 99.

Manuscript Accepted by the Society 13 December 2006

Printed in the U.S.A.